Abstracts, Division of Biological Chemistry, 197th National Meeting of the American Chemical Society, April 9–14, 1989

R. David Cole, Chairman; Perry A. Frey, Chairman Elect;
JoAnne Stubbe, Program Chairman; David S. Sigman, Program Chairman Elect

MONDAY MORNING—SYMPOSIUM ON DNA DAMAGE—L. HURLEY, ORGANIZER, PRESIDING

1. DNA, Light, and Cancer. *J.-S. Taylor*. Department of Chemistry, Washington University, St. Louis, MO 63130.

Approximately 1 of 10 Americans will contract skin cancer in their lifetime. The correlation between sunlight and skin cancer comes from two pieces of evidence: (1) exposure of DNA to sunlight leads to the formation of photoproducts and (2) victims of the DNA repair disorder xeroderma pigmentosum have an approximately 1000-fold higher chance of developing skin cancer. Though many photoproducts have been identified, little is known about the solution-state structure and properties of DNA containing such photoproducts and how this relates to their lethality, mutagenicity, and carcinogenicity. The inability to derive such structure–activity relationships is principally due to the lack of methods for the preparation of pure, well-characterized, photoproduct-containing DNA for study. We are approaching this problem by synthesizing building blocks for the sequence-specific introduction of photoproducts into oligonucleotides by solid-phase DNA synthesis technology. These oligonucleotides are then used to construct DNA duplexes for high-field NMR, biophysical, enzymological, and in vivo mutagenesis studies. The talk will focus on the structure–activity relationships of cis-syn, trans-syn, 6-4, and Dewar dipyrimidine photoproducts.

2. Conformational Aspects of DNA Degradation by Bleomycin. *J. W. Kozarich*, C. R. Krishnamoorthy, L. Worth, Jr., L. Rabow, G. McGall, and J. Stubbe. Department of Chemistry and Biochemistry, University of Maryland, College Park, MD 20742, and Department of Chemistry, Massachusetts Institute of Technology, Cambridge, MA 02139.

In the presence of Fe(II) and O_2, bleomycin is capable of cleaving both B-form and A-form structural motifs. Moreover, the increased accessibility of minor groove hydrogens in the A-form leads to an alteration in the chemistry of cleavage. Specifically, B-form structures are cleaved predominantly by 4′-hydrogen abstraction, while A-form structures appear to undergo abstraction at both the 4′- and 1′-positions. We have recently performed an extensive investigation of cleavage by bleomycin of a variety of defined DNAs and DNA–RNA hybrids in order to test this hypothesis. In addition, we have used isotopically labeled DNAs (^2H and ^3H) to probe differences in chemical mechanism between these two forms. Our findings will be discussed. (Supported by NIH Grant GM 34454.)

3. Bistranded Oxidative DNA Sugar Damage by Targeted Neocarzinostatin Radicals. *I. H. Goldberg*, L. S. Kappen, D.-H. Chin, A. Galat, and S. H. Lee. Department of Biological Chemistry and Molecular Pharmacology, Harvard Medical School, Boston, MA 02115.

The nonprotein chromophore of the antitumor antibiotic neocarzinostatin binds DNA by intercalation, placing its novel, highly strained bicyclic ene-diyne-containing core in the minor groove of B-DNA. Upon activation (by thiol or sodium borohydride) the core structure rearranges to form a diradical that abstracts hydrogen atoms from deoxyribose of the DNA backbone. Single-strand breaks found mainly at T residues result from drug attack at C-5′ of deoxyribose to form predominantly nucleoside 5′-aldehyde. At certain sequences, such as d(AGC), abasic sites are produced at the C residue by radical attack at C-1′ to form 2-deoxyribonolactone with intact phosphodiester linkages, in addition to direct strand breaks at the T residue located two nucleotides to the 3′-side on the complementary strand, resulting in bistranded lesions directly across the minor groove from each other. Biochemical, ^1H NMR, MS, and molecular modeling studies supporting these mechanisms and the implications of the bistranded lesion for cell death and mutagenesis will be described.

4. Calicheamicin γ_1^I and DNA: Molecular Recognition Process Responsible for Site Specificity. *Nada Zein* and George A. Ellestad. Infectious Disease Research Section, Medical Research Division, Lederle Laboratories, American Cyanamid Company, Pearl River, NY 10965.

An important aspect of the phenomenally potent diyne-ene-containing antitumor agent calicheamicin γ_1^I is its remarkable double-stranded DNA cleaving properties at specific sites. Our studies suggest that a nondiffusible 1,4-dehydrobenzene diradical species initiates oxidative strand scission by hydrogen abstraction from the deoxyribose ring. Cleavage experiments on restriction fragments as well as synthetic oligomers show that calicheamicin interacts with the DNA in a unidirectional manner. Moreover, the specificity of this cleavage is attributed to a unique minor groove association with the drug thiobenzoate-carbohydrate tail followed by partial insertion of the diyne-ene moiety into the groove at sites where local helix parameters are optimal. A computer-generated model illustrates the molecular encounter between the drug and the genetic material.

MONDAY AFTERNOON—SYMPOSIUM ON DNA REPAIR—J. A. GERLT, ORGANIZER, PRESIDING

5. Enzymological and Chemical Properties of Aldehydic Abasic Sites. Abhijit Mazumder, Muthiah Manoharan, Lois Rabow, Joyce A. Wilde, JoAnne Stubbe, Philip H. Bolton, and *John A. Gerlt*. Department of Chemistry and Biochemistry, University of Maryland, College Park, MD 20742, Department of Chemistry, Massachusetts Institute of Technology, Cambridge, MA 02139, and Department of Chemistry, Wesleyan University, Middletown, CT 06457.

Aldehydic abasic sites in synthetic heteroduplexes can be conveniently prepared by the action of uracil-DNA glycosylase on strands containing deoxyuridine residues. By use of this approach, abasic sites specifically labeled with ^{13}C in the

0006-2960/89/0428-1931$01.50/0

aldehydic carbon and with ^{17}O in the aldehydic and hemiacetal oxygens have been prepared, and ^{13}C and ^{17}O NMR spectroscopies have been used to quantitate the amounts of the aldehydic and hemiacetal forms. The mechanism of the reaction catalyzed by UV endonuclease V from bacteriophage T_4 has been studied with abasic sites labeled with ^3H and ^{13}C and found to proceed by stereospecific β-elimination of the 3′-phosphate group.

6. DNA Photolyases from *E. coli* and Yeast: Action Mechanism and Interaction with Other DNA Repair Pathways. *Gwendolyn B. Sancar.* Department of Biochemistry, School of Medicine, University of North Carolina at Chapel Hill, Chapel Hill, NC 27599-7260.

During the past 5 years application of recombinant DNA technology has yielded quantities of photolyase from *E. coli* and *Saccharomyces cerevisiae* sufficient for detailed studies on the mechanisms of substrate recognition and dimer photolysis. Such studies have revealed that these enzymes bind their substrates with a discrimination similar to that of sequence-specific DNA binding proteins. The enzymes approach the dimer from the major groove in double-stranded DNA and bind to a face of the helix defined by a limited number of phosphodiester bonds 5′ and 3′ to the dimer and by C4–C6 of the dimer. Both enzymes contain two intrinsic, noncovalently bound chromophores, $FADH_2$ and 5,10-methenyltetrahydrofolate. Photolysis of the dimer proceeds via electron donation by an excited state of the flavin chromophore to the dimer; energy for this reaction is supplied primarily by the folate chromophore, which acts as a light harvester for the enzyme and transfers energy to $FADH_2$. In both organisms photolyase makes an important contribution to the dark repair of pyrimidine dimers by stimulating the incision step of nucleotide excision repair.

7. DNA Repair Enzymes for Radical-Damaged Deoxyribose. *Bruce Demple.* Department of Biochemistry and Molecular Biology, Harvard University, Cambridge, MA 02138.

Lesions to deoxyribose are prominent among the many damges formed in DNA by free radicals, such as those produced by ionizing radiation or the Fenton reaction. Such lesions may either block DNA 3′ termini and prevent repair synthesis by DNA polymerase I or exist as oxidized deoxyribose residues in intact chains and block DNA replication. Removal of these damages is essential for cellular recovery after oxygen radical attack on DNA. We have characterized the enzymes that initiate this repair in several organisms—the bacterium *Escherichia coli*, the yeast *Saccharomyces cerevisiae*, and cultured human cells. The mechanisms and cellular roles of these enzymes will be discussed.

8. Enzymology of Methyl-Directed DNA Mismatch Correction. Karin Au, Deani Cooper, Michelle Grilley, Robert Lahue, Shin-San Su, Katherine Welsh, and *Paul Modrich.* Department of Biochemistry, Duke University Medical Center, Durham, NC 27710.

DNA biosynthetic errors in *E. coli* are subject to postreplication repair by the methyl-directed mismatch correction system. Repair by this system responds to the state of methylation of d(GATC) sequences, with correction directed to the newly synthesized strand by virtue of its transient undermethylation. This reaction has been reconstituted in vitro by using eight near homogeneous activities: mutH, mutL, and mutS gene products, DNA helicase II, SSB, DNA polymerase III holoenzyme, DNA ligase, and a 55-kDa stimulatory protein. The defined system is capable of recognition and correction of seven of the eight possible base–base mispairs (all except C-C) and responds in a dramatic fashion to the state of d(GATC) methylation, with the state of modification of a single d(GATC) site located 1000 base pairs from the mismatch being sufficient to direct repair. We have found that mutS protein binds to mismatched base pairs and that mutH protein possesses a weak d(GATC) endonuclease activity which incises an unmethylated DNA site. This endonuclease undergoes activation in a reaction that is dependent on mutL and mutS proteins, ATP, and the presence of a mismatch within the substrate. These findings indicate that strand specificity of correction is determined by the strand specificity of mutH-promoted incision.

TUESDAY MORNING—AWARDS SYMPOSIUM—D. COLE, PRESIDING

Bader Award Address

9. No abstract available.

Repligen Award Address

10. Functioning of DNA Polymerases. *Stephen J. Benkovic.* Department of Chemistry, The Pennsylvania State University, 152 Davey Laboratory, University Park, PA 16802.

Kinetic schemes describing the polymerization of correct and incorrect dNTPs by the Klenow fragment of DNA polymerase I have been developed by using both short DNA oligomers of defined sequence and primed M-13. The high polymerase fidelity arises from a three-stage mechanism: (1) a dramatic reduction in the rate of phosphodiester bond formation in the case of incorrect vs correct nucleotides; (2) a weak editing function furnished by the 3′ → 5′ exonuclease; and (3) a sharp reduction in the rate of polymerization onto a mismatch 3′-terminus. These kinetic studies have been complemented by studies on the structure of the DNA–enzyme–dNTP complex using fluorescence energy-transfer methods as well as employing substituted oligomers that contain a cross-link between the base pairs or possess a photoactivatable label. The latter methods have provided a view of the ternary reactive complex for the Klenow fragment superimposed on the framework established by X-ray crystallography [Ollis et al. (1985) *Nature 313*, 762] as well as of the importance of strand separation in the operation of this and other polymerases.

Ipatieff Award Address

11. Enzymatic Catalysis in Organic Solvents. *Alexander M. Klibanov.* Department of Chemistry, Massachusetts Institute of Technology, Cambridge, MA 02139.

Enzymatic catalysis in nonaqueous media has progressed from using enzymes in aqueous solutions containing relatively low fractions of water-miscible organic cosolvents to that in biphasic aqueous–organic mixtures, to that in microemulsions and reversed micelles, to that in monophasic organic media containing small amounts of water, to that in anhydrous organic solvents. It is easy to understand why enzymes retain catalytic activity in the first three types of reaction media, for in all of them the enzyme molecules are located in aqueous environments (and therefore the inherent enzymatic properties

in such systems are usually not significantly different from those in water). Conversely, the phenomenon of enzymes vigorously functioning in monophasic organic solvents with little or no water goes against the conventional wisdom and universally accepted dogmas. Nevertheless, it has now been firmly established that this phenomenon exists, that it is quite general, and that enzymes in organic solvents exhibit striking novel properties. In this presentation some fundamental questions concerning enzyme action in nonaqueous media will be addressed.

TUESDAY AFTERNOON—PFIZER AWARD SYMPOSIUM—S. J. BENKOVIC, PRESIDING

12. Solving Enzyme Mechanisms by Transient Kinetics. *Kenneth A. Johnson.* Molecular and Cell Biology, The Pennsylvania State University, University Park, PA 16802.

Recent advances in transient kinetic methods have led to definition of the complete reaction sequence for four enzymes: the microtubule-dynein ATPase, dihydrofolate reductase (DHFR), DNA polymerase I, and enolpyruvoylshikimate-3-phosphate (EPSP) synthase. In each case the reaction mechanism was established by direct measurement of the events occurring at the enzyme active sites, leading a complete free energy profile for the reaction pathway. Kinetic analysis of the microtubule-dynein ATPase defined the pathway and thermodynamics of energy transduction for force production for microtubule-dependent movements. In work on DHFR, stopped-flow fluorescence energy transfer was used to directly measure the rate of the chemical reaction at the active enzyme site and led to a complete kinetic scheme which formed the basis to quantitatively evaluate active-site mutants. Studies on DNA polymerase I established the elementary steps in the reaction sequence accounting for the fidelity of template-directed synthesis of DNA. Finally, work on EPSP synthase, in collaboration with Karen S. Anderson (Monsanto), provided a complete description of the pathway and led to the isolation and characterization of a tetrahedral intermediate formed at the active site of the enzyme. Each study illustrates the use of modern transient kinetic methods to establish the pathway of an enzymatic reaction by direct measurement. (Supported by NIH GM26726.)

13. Mechanism of Coupling of ATP Hydrolysis to the Transport of Ca^{2+}. *William P. Jencks.* Graduate Department of Biochemistry, Brandeis University, Waltham, MA 02254.

An understanding of the mechanism by which ATP hydrolysis is coupled to active transport by the Ca-ATPase of sarcoplasmic reticulum and other transport ATPases requires an understanding of changes in catalytic and vectorial specificities during the reaction cycle, which define the coupling. These specificity rules divide the chemical (ATP hydrolysis) and vectorial (Ca^{2+} transport) processes each into two parts, which alternate in the reaction cycle so that neither overall process can occur unless the other also occurs. Mechanisms by which these changes in specificity take place will be reviewed. The change in catalytic specificity that allows phosphorylation by ATP occurs only after the binding of two Ca^{2+} ions, and the change that allows reaction of E-P with water occurs only after both Ca^{2+} have dissociated inside the vesicle. The change in vectorial specificity for Ca^{2+} dissociation binding occurs in a very rapid phosphorylation step ($k \geq 1000$ s^{-1}) after one or more rate-limiting conformational changes that are induced by Ca^{2+} and ATP.

14. Actomyosin ATPase and the Mechanism of Muscle Contraction. *Edwin W. Taylor.* Department of Molecular Genetics and Cell Biology, University of Chicago, 920 E. 58th Street, Chicago, IL 60637.

A kinetic scheme for actomyosin ATPase is

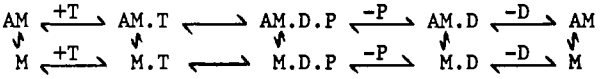

where A is fibrous actin, M is a myosin head, and T, D, and P are ATP, ADP, and phosphate, respectively. M·T and M·D·P are in rapid equilibrium with actin on the time scale of the steady-state hydrolysis cycle. Activation of ATPase activity by actin arises from a large increase in the rate of dissociation of D and P from AM·D·P relative to M·D·P. The scheme is derived from kinetic studies in solution. Studies with myofibrils, which preserve the essential structural features of muscle, have given similar values for rate constants for the ATP binding and actin dissociation steps, the hydrolysis step, and the steady-state rate. Relative motion (contraction) is determined by the rate constants of product dissociation. The scheme provides a basis for quantitative models of the contraction cycle.

WEDNESDAY MORNING—SYMPOSIUM ON CATALYTIC ANTIBODIES (SECTION A)—S. J. BENKOVIC, ORGANIZER, PRESIDING

15. Antibody Catalysis. *Richard A. Lerner.* Department of Molecular Biology, Research Institute of Scripps Clinic, 10666 North Torrey Pines Road, La Jolla, CA 92037.

The immune system consists of the most diversified set of binding proteins known in biology. Recently this binding energy has been exploited to catalyze a variety of chemical transformations including hydrolytic, concerted, and bimolecular reactions. We will report our progress in making new antibody catalysts, including those which enhance the rate of hydrolysis of the amide bond. The advent of catalytic antibodies promises new catalysts that extend the range of catalysis by proteins to chemical transformations that were not required during the evolution of enzyme.

16. New Strategies for the Design of Catalytic Antibodies. *P. G. Schultz.* Department of Chemistry, University of California, Berkeley, CA 94720.

A number of strategies have been developed whereby the high binding affinity and specificity of antibodies can be exploited in the design of novel catalysts with tailored specificities. The binding energy of antibodies to specific recognition elements has been used to selectively stabilize transition-state configurations on reaction pathways or to overcome entropic barriers involved in orienting reaction partners. Antibody-hapten complementarity has been exploited to introduce catalytically active side chains into antibody combining sites, and antibodies have been generated with cofactor binding sites. Antibody combining sites have also been selectively modified with synthetic catalytic groups to produce semisynthetic catalytic antibodies, and site-directed mutagenesis is currently being applied to the development of catalytic antibodies. By use of these approaches, antibodies have been shown to selectively catalyze several classes of reactions, including transacylation, elimination, Schiff base formation, pericyclic, redox, and photochemical reactions.

17. Antibody-Catalyzed Concerted Chemical Reactions. *Donald Hilvert*. Department of Molecular Biology, Research Institute of Scripps Clinic, 10666 North Torrey Pines Road, La Jolla, CA 92037.

Recent attention has focused on the mammalian immune system as a source of highly specific, tailored catalysts. The construction of enzyme-like antibodies involves synthesizing compounds that mimic the transition-state structure of a particular reaction, eliciting an immune response against such substances, and screening the resulting immunoglobulins for the desired activity. Because concerted chemical reactions are expected to be sensitive to induced strain and proximity considerations and because they do not require the participation of specifically oriented catalytic groups within the binding pocket, they are especially suited for catalysis by antibodies. Such processes are, moreover, of enormous practical and theoretical interest. Our progress in generating immunoglobulins that catalyze concerted chemical reactions, particularly sigmatropic rearrangements and Diels–Alder cyclization, will be discussed.

18. Catalytic Antibodies. *Stephen J. Benkovic*, Andrew D. Napper, Kim Janda, and Richard A. Lerner. Department of Chemistry, The Pennsylvania State University, University Park, PA 16802, and Scripps Institute, La Jolla, CA 92037.

Monoclonal antibodies have been elicited to transition-state analogues that are capable of catalyzing (i) a stereospecific 6-membered ring cyclization, (ii) a stereospecific bimolecular aminolysis reaction, and (iii) a hydrolysis of an aromatic amide. Examination of the kinetics of these reactions reveals that these reactions have much in common with enzyme-catalyzed processes in that they follow Lineweaver–Burk kinetics, show high enantioselectivity, and in the presence of the eliciting hapten show tight binding competitive inhibition. The rate acceleration observed in the presence of antibody relative to the spontaneous reaction may be predicted from the values of the binding constants for the substrate versus that of the eliciting hapten. Ratios that lie above this range suggest the presence of catalytic functionality in the antibody binding site. Given the behavior of the presently known systems, some predictions can be made about the nature of reactions that would be particularly sensitive to antibody catalysis.

WEDNESDAY MORNING—SYMPOSIUM ON PEROXIDASES (COSPONSORED WITH THE DIVISION OF MICROBIAL AND BIOCHEMICAL TECHNOLOGY) (SECTION B)—M. TIEN, ORGANIZER, PRESIDING

19. Raman Spectroscopy of Intermediates in Heme Protein Catalysis. *G. T. Babcock*, W. A. Oertling, R. Kean, C. Varotsis, A. Salehi, and C. K. Chang. Department of Chemistry, Michigan State University, East Lansing, MI 48824-1322.

Cytochrome oxidase catalyzes the four-electron reduction of oxygen to water; peroxidases can be considered to catalyze the second half of this reaction as they use peroxide as a substrate and produce water. From a chemical point of view, these reactions are complex: the oxygen–oxygen bond must be broken, oxygen–hydrogen bonds must be formed, and these reactions must take place such that potentially damaging intermediates are not released into the cell. Time-resolved resonance Raman spectroscopy has the potential to probe the mechanism of these reactions, and we have used this technique to study both the reactions of cytochrome oxidase and of several peroxidases with their oxygenic substrates. Characterizing the intermediates that occur in these processes requires a model compound study of likely structures. To this end, we have prepared ferrous oxy, ferryl oxo, and metalloporphyrin π-cation radicals and studied them in detail by vibrational spectroscopy. The results of these enzyme and model compound experiments will be discussed.

20. NMR Studies of the Molecular and Electronic Structure of Heme Peroxidases. *Gerd N. La Mar*, V. Thanabal, and Jeffrey S. de Ropp. Department of Chemistry, University of California, Davis, CA 95616.

We have utilized a number of nuclear magnetic resonance (NMR) techniques to probe the active-site environment of a variety of heme peroxidases including horseradish peroxidase (HRP), bovine lactoperoxidase (LPO), and lignin peroxidase (LiPO). Direct detection of ^2H NMR of isotope-labeled hemin reconstituted into HRP has confirmed that the resting state is five coordinate and does not possess a bound water molecule. The location of the *meso*-proton hyperfine-shifted peaks in HRP compound I supports an a_{1u} rather than an a_{2u} description for the porphyrin cation radical orbital ground state. The low-spin HRP–CN complex has yielded a very informative 2D NOESY map which confirms previous assignments of resonances to heme pocket residues. Nuclear Overhauser effect (NOE) studies have also been extended to LPO–CN which confirm the unusual functionalization of the 8-methyl group (8-thiolmethylene group) and suggest that the active site, as in HRP and cytochrome *c* peroxidase, possesses both a distal Arg and His, as well as a bound proximal His which exhibits extensive imidazolate character.

21. Structural Studies on Cytochrome *c* Peroxidase. Steven L. Edwards and *Thomas L. Poulos*. Center for Advanced Research in Biotechnology, 9600 Gudelsky Drive, Rockville, MD 20850.

Crystallographic studies on CCP have progressed on three fronts: examining the conformational dynamics of CCP using a series of ligands (F^-, CN^-, and NO) to prove the active site; attempts to determine the X-ray structure of the CCP–cyt *c* complex; and the crystal structure of CCP compound I. The structure of various ligated complexes of CCP have revealed some unexpected conformational effects. The most notable is that NO binding to ferric CCP on the distal side of the heme results in a conformational change in a Trp residue on the proximal side of the heme. This suggests a long-range electronic coupling between the heme and proximal side residues. Other observed changes include distal side residues which adjust to optimize hydrogen-bonding interactions with the ligand. CCP–cyt *c* crystals diffract to about 3.2 Å and contain both a CCP and cyt *c* molecule, yet only the CCP molecules are visible in the electron density map. This suggests a dynamical or static disordering of cyt *c* relative to CCP. Finally, the crystal structure of compound I has been determined at −15 °C and has confirmed the presence of the ferryl oxygen atom and motion of the iron into the porphyrin core. (Work supported in part by NSF Grant DMB-8716316.)

22. Structures and Mechanisms of Peroxidases. *Paul R. Ortiz de Montellano*. Department of Pharmaceutical Chemistry, School of Pharmacy, University of California, San Francisco, CA 94143-0446.

Studies of the active-site architecture of horseradish peroxidase using mechanism-based inactivating agents have led to the postulate that substrates interact with the heme edge

rather than the ferryl oxygen of classical peroxidases. The interaction of substrates with the enzyme specifically involves the heme edge in the vicinity of pyrrole ring D. Recent studies of other peroxidases indicate that the basic elements of the proposed active-site architecture are fairly general. The mechanisms by which the peroxidases are inactivated provide further insights into the catalytic process and will be discussed. (Work supported by NIH Grant GM 32488.)

WEDNESDAY AFTERNOON—ELI LILLY AWARD SYMPOSIUM (SECTION A)—W. JENCKS, PRESIDING

23. recA Protein Mediated DNA Strand Exchange. *Michael M. Cox*. Department of Biochemistry, University of Wisconsin, Madison, WI 53706.

The recA protein of *E. coli* promotes an exchange of strands between homologous DNA molecules. The reaction proceeds in several phases: (1) formation of an extended recA nucleoprotein filament covering a DNA molecule (DNA1) that must be at least partially single stranded, (2) homologous alignment of DNA1 with a second DNA (DNA2) to form a paranemic joint, (3) conversion of the paranemic joint to a plectonemic joint to initiate strand exchange, and (4) a unidirectional branch migration reaction coupled to ATP hydrolysis. Several key features of this reaction are not understood, including the structural relationship of DNA1 and DNA2 in the paranemic complex and the molecular role of ATP hydrolysis. Recent data on these aspects of the problem will be presented along with a model that accounts for the reaction energetically and structurally.

24. Underwound DNA in Solution Adopts a Superhelical Form. H. Benjamin, C. Boles, *N. Cozzarelli*, C. Donahue, P. Droege, J. Dungan, R. Kanaar, P. van de Putte, S. Wasserman, and J. White. Department of Molecular Biology, University of California, Berkeley, CA 94720.

Using topological methods and electron microscopy, we have determined the major structural parameters of superhelical DNA as a function of degree of underwinding. The biological implications will be discussed, particularly the role of supercoiling in site-specific recombination by resolvases and invertases.

25. Enzymes Required for Herpes Simplex 1 Replication. *I. R. Lehman*. Department of Biochemistry, Stanford University School of Medicine, Stanford, CA 94305-5307.

Seven genes in the herpes simplex 1 (HSV-1) genome are necessary and sufficient for the replication in trans of plasmids containing an HSV-1 origin (ori_S). The function in replication of the products of two of these genes had previously been identified as the HSV-1 DNA polymerase and single-stranded DNA binding protein. We have now identified and purified to homogeneity (i) an 82-kDa origin-specific binding protein (ori_S binding protein) and (ii) a DNA helicase-primase consisting of three subunits with M_r's of 120 000, 97 000, and 70 000. The ori_S binding protein is very likely necessary for the initiation of HSV-1 DNA replication, and the DNA helicase-primase may prime lagging strand synthesis as it unwinds DNA at the viral replication fork.

26. Multiple DNA Binding Modes and Cooperativities of the *E. coli* Single-Strand Binding Protein. *Timothy M. Lohman*. Department of Biochemistry and Biophysics, Texas A&M University, College Station, TX 77843.

The *E. coli* SSB protein, a helix-destabilizing protein, is required for replication, recombination, and some repair processes in vivo. It is a stable tetramer in solution that binds to ss DNA in a number of different binding modes and with different positive cooperativities between DNA-bound tetramers in vitro. Furthermore, there is a dramatic negative cooperativity for binding ss DNA among the ss DNA binding sites within individual SSB tetramers, and this negative cooperativity is involved in the modulation of the ss polynucleotide binding modes in vitro. These multiple interactions of the SSB protein with ss nucleic acids will be discussed, as well as their possible relationship to the different functions of the SSB protein in vivo.

WEDNESDAY AFTERNOON—SYMPOSIUM ON RATIONAL TARGETS FOR HERBICIDE DESIGN (COSPONSORED WITH THE DIVISION OF AGROCHEMICALS) (SECTION B)—P. HAYWORTH, ORGANIZER, PRESIDING

Inhibition of Acetyl-CoA Carboxylase by Two Classes of Grass-Selective Herbicides. *Alan R. Rendina*, Jacqueline D. Beaudoin, Adrienne C. Craig-Kennard, and Judy M. Felts. Chevron Chemical Company, Richmond, CA 94804.

The selective grass herbicides diclofop (I), haloxyfop, trifop (aryloxyphenoxypropionates), alloxydim, sethoxydim, and clethodim (II) (cyclohexanediones) are potent, reversible inhibitors of acetyl-CoA carboxylase (ACC) partially purified from barley, corn, and wheat. Inhibition by I and II is noncompetitive vs MgATP and HCO_3^- with $K_{is} \approx K_{ii}$ and acetyl-CoA with $K_{is} < K_{ii}$. Of the two biotin-dependent partial reactions, only the acetyl-CoA $\rightleftharpoons$ malonyl-CoA exchange is significantly inhibited by I and II, suggesting that the herbicides interfere with the carboxyltransferase site rather than the biotin carboxylase site. Multiple inhibition studies produce parallel lines ($1/v$ vs [II] at fixed [I]), suggesting that binding of both herbicide classes is mutually exclusive. K_{is} values range from 0.01 to 1.4 μM, depending on the grass (diclofop < clethodim $\approx$ haloxyfop $\approx$ trifop < sethoxydim < alloxydim). For wheat the K_{is} of (*R*)-(+)-trifop is 1.98 $\pm$ 0.22 times lower than the racemic mixture, confirming the stereoselectivity observed in the plant. ACC from broadleaf plants (spinach and mung bean) is much less sensitive to inhibition by these herbicides (K_{is} = 16 μM–2.2 mM). These results identify ACC as the site of action for both herbicide classes and may explain their selectivity for monocotyledonous species.

Interactions of Imidazolinones with AHAS from Plants. *D. Shaner*, B. Singh, K. Newhouse, M. Stidham, and G. Schmitt. American Cyanamid Company, Princeton, NJ 08540.

Imidazolinones are a new class of herbicides that kill plants by inhibiting acetohydroxyacid synthase (AHAS). Although plant species vary in their sensitivity to the imidazolinones and in the level of extractable AHAS activity, there does not appear to be any relationship between a plant's herbicidal sensitivity and AHAS activity. Two different forms of AHAS have been isolated from Black Mexican sweet corn suspension cells. One form is inhibited by Val, Leu, and Ile and by imidazolinones, while the other is hypersensitive to imidazolinones but completely insensitive to the branched-chain amino acids. Imidazolinones treatment also causes a rapid decrease in the levels of extractable AHAS activity, indicating some type of slowly reversible binding to the enzyme in vivo. Sulfometuron methyl, another potent inhibitor of AHAS, treatment does not cause a decrease in the levels of extractable AHAS and can protect AHAS activity in vivo from the in-

hibitory effects of imidazolinones. However, imidazolinone-resistant corn lines, which have been found through cell culture selection, are not all sensitive to sulfonylureas. These results suggest that while these two classes of herbicides share some AHAS binding site in common, they do not share identical binding sites.

EPSP Synthase: Isolation and Kinetic Characterization of an Intermediate in the Enzyme Reaction Pathway. *Karen S. Anderson*, Kenneth A. Johnson, Alan J. Benesi, and James A. Sikorski. Monsanto Agricultural Products, St. Louis, MO 63167, and The Pennsylvania State University, University Park, PA 16802.

EPSP (5-enolpyruvoylshikimate-3-phosphate) synthase catalyzes the transfer of an enolpyruvoyl moiety from phosphoenolpyruvate (PEP) to shikimic acid 3-phosphate (S3P). The enzyme is inhibited by the commercially important herbicide glyphosate. The enzyme reaction mechanism was investigated by rapid chemical quench-flow studies. These studies have established the enzyme reaction as an addition–elimination mechanism proceeding via a tetrahedral intermediate (I) formed by the nucleophilic attack of the 5-OH

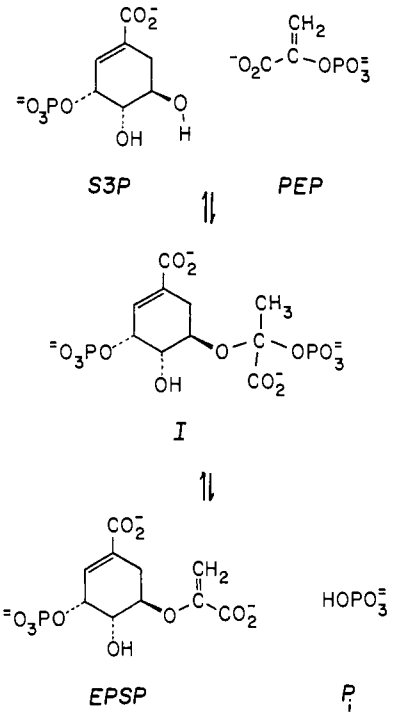

of S3P on the C-2 of PEP as shown. The tetrahedral structure suggested as an intermediate has been confirmed by isolation and NMR characterization. The mechanistic aspects of EPSP synthase including the kinetics, isolation, and structural elucidation of the tetrahedral intermediate will be discussed. In addition, the mode of inhibition by glyphosate will be addressed. (Supported in part by NIH Grant GM26726 to K.A.J.)

From Herbicides to Enzymes and Back Again. *John V. Schloss* and Ann Aulabaugh. Central Research and Development Department, Experimental Station E328, E. I. du Pont de Nemours and Company, Wilmington, DE 19898.

Inhibition of acetolactate synthase, the first common enzyme of branched-chain amino acid biosynthesis, by various herbicides (sulfonylurea, imidazolinone, and triazolopyrimidine or sulfonanilide) results in the death of plants rather than the simple inhibition of growth due to the limitation of valine, leucine, and isoleucine. Of the three common enzymes in this pathway, which also includes ketol-acid reductoisomerase and dihydroxyacid dehydratase, genetic evidence suggests that inhibition of the former (but not the latter) enzyme might also be herbicidal. Potent inhibitors of the reductoisomerase, which are analogues of the rearrangement transition state, have been obtained by de novo design. These selective inhibitors of the reductoisomerase are herbicidal and bacteriostatic, similar to the properties of the acetolactate synthase inhibitors.

Wednesday Afternoon—Symposium on Peroxidases (Cosponsored with the Division of Microbial and Biochemical Technology) (Section C)—A. Pakora, Organizer, Presiding

Peroxidases: Studies in Thrills and Chills. *Saul L. Neidleman.* Cetus Corporation, 1400 53rd Street, Emeryville, CA 94608.

Peroxidases have enormous synthetic versatility. Personal involvement with these enzymes has afforded a number of exciting discoveries. These include the synthesis of heterogeneous dihalides such as bromochloro- and fluoroiodopropanols; the isolation of a hydrogen peroxide resistant, non-heme chloroperoxidase; and the oxidative and peroxidative synthesis of ethylene from a natural plant precursor, 1-aminocyclopropane-1-carboxylic acid. In studies directed at peroxidase modification of the tetracycline antibiotics, it was noted that low temperature (6–9 °C) inhibited oxidative cleavage of the 4-dimethylamino moiety from the molecule, but allowed the desired 9-hydroxylation reaction to occur, in contrast to room temperature, which favored the 4-dimethylamino cleavage, in conjunction with the 9-hydroxylation. The chill favored production of the desired 9-hydroxylated derivative.

Analytical Applications of Horseradish Peroxidase. *T. T. Ngo.* Department of Developmental Cell Biology, University of California, Irvine, CA 92717.

Horseradish peroxidase (HRP) is a hemoglycoprotein of 40 000 molecular weight with heme as the cofactor. Carbohydrate accounts for 18% of its total mass. There are seven known isozymes. HRP catalyzes the oxidation by a peroxide of a number of aromatic compounds (hydrogen donors). Reactions catalyzed by HRP can be monitored by colorimetric, fluorometric, or chemiluminometric methods. The substrates for these reactions will be described. Analytical applications of HRP include the detection of hydrogen peroxide, measurement of metabolites when used in conjunction with specific oxidases, its use as label in immunoassay, and its use in temperature abuse sensor. Representative examples for the analytical uses of HRP will be discussed.

Unusual Catalytic Activities of Peroxidases. *Jonathan S. Dordick*, Mark Schmall, and Keungarp Ryu. Chemical and Materials Engineering Department, University of Iowa, Iowa City, IA 52242.

Unusual catalytic activities of peroxidases have been studied in both aqueous and organic media. The catalytic activity of horseradish peroxidase (HRP) is often stimulated in nonaqueous media; enhancements in turnover number of nearly 6-fold have been found in a wide variety of solvents compared to that in water. The solvent also alters the substrate specificity of HRP; hydrophobic substrates such as *p*-cresol and *p*-propylphenol activate HRP in hydrophobic solvents to a

greater degree than in hydrophilic substrates. We have also studied lignin peroxidase (LiP) catalysis in aqueous solutions. LiP catalyzed the dihydroxyfumaric acid dependent, H_2O_2-independent hydroxylation of phenols. This reaction appears to be hydroxyl radical dependent and is similar to the previously described HRP-catalyzed hydroxylation reaction. This reaction represents the first true monooxygenase reaction known for LiP.

Polymerization of Phenols Catalyzed by Peroxidase: Controls and Applications. A. R. Pokora and *W. L. Cyrus, Jr.* Mead Central Research, Chillicothe, OH 45601.

Enzyme catalysis in organic solvents is an area of research holding great promise for industrial processes. Horseradish peroxidase catalyzes the oxidative coupling of phenols in a variety of aqueous–organic solvent mixtures. Utilizing these solvent mixes helps overcome low substrate solubilities, facilitates recovery of the product, and plays a key role in controlling the molecular weight of the product. The oxidative coupling of phenols catalyzed by peroxidase has been explored not only as a potential substitute for phenol–formaldehyde resins but as an attractive alternative to traditional chemical oxidative coupling reactions.

Biomechanical Pulping of Wood: Results with a Model Process. *G. F. Leatham*, G. C. Myers, T. W. Wegner, I. B. Sachs, D. J. Cullen, and T. K. Kirk. USDA Forest Products Laboratory, Madison, WI 53705.

The lignin peroxidases produced by white-rot basidiomycetes have potential importance in a number of industrial applications. One application of potential large-scale impact to the paper and pulp industry is biomechanical pulping. This is where white-rot fungi are allowed to permeate and partially degrade wood chips with secreted enzymes that include ligninases after which mechanical pulp is made. This fungal pretreatment has several benefits as well as potential advantages over the chemical pretreatments currently in use. The fungal pretreatments can greatly decrease the energy requirements for producing pulp in mechanical refiners, improve paper strength properties, and decrease the amount of environmentally undesirable chemicals required to produce pulp via chemimechanical processes. Here we discuss the design of a model biomechanical pulping process and some of the results obtained in its evaluation.

Ligninases from White-Rot Fungi Can Degrade Hazardous Chemicals. *T. W. Joyce*, Hou-min Chang, and Yin Caifant. Department of Wood and Paper Science, North Carolina State University, Box 8005, Raleigh, NC 27695.

The wood-decaying, white-rot fungus *Phanerochaete chrysosporium* secretes a family of enzymes that are able to degrade not only lignin, the enzyme substrate in nature, but also a wide variety of hazardous chemicals. We have found that the fungus can be immobilized in a reactor and used in a waste treatment system. Using this treatment system, we have been able to degrade such compounds as pentachlorophenol, dioxin, and trinitrotoluene (TNT).

WEDNESDAY AFTERNOON—SYMPOSIUM ON MOLECULAR ARCHITECTURE: DESIGN, SYNTHESIS, AND FUNCTION OF SUPRAMOLECULAR STRUCTURES (CROSS-LISTED WITH THE DIVISION OF CHEMICAL EDUCATION) (SECTION D)—D. GUTSCHE, ORGANIZER, PRESIDING

THURSDAY MORNING—SYMPOSIUM ON CHOLESTEROL METABOLISM AND DISEASE (COSPONSORED WITH THE DIVISION OF MEDICINAL CHEMISTRY) (SECTION A)—D. POULTER, ORGANIZER, PRESIDING

27. Lipoprotein Receptors: Molecular Machines That Lower Blood Cholesterol. *Joseph L. Goldstein* and Michael S. Brown. Department of Molecular Genetics, University of Texas Southwestern Medical Center, Dallas, TX 75235.

The low-density lipoprotein (LDL) receptor is a cell surface protein that mediates the removal of cholesterol-carrying lipoproteins from blood and thereby helps to control the concentration of blood cholesterol. When LDL receptors are deficient, as a result of genetic or acquired abnormalities, LDL builds up in blood and atherosclerosis ensues. The structure, function, and feedback regulation of the LDL receptor gene will be discussed.

28. Isopentenyl Diphosphate Isomerase. Enzymology and Mechanism of Action. *C. Dale Poulter.* Department of Chemistry, University of Utah, Salt Lake City, UT 84112.

Isopentenyl diphosphate isomerase catalyzes the rearrangement of isopentenyl diphosphate (IPP) to dimethylallyl diphosphate (DMAPP) by a [1.3]hydrogen shift. The product of the reaction is a potent electrophile that serves as the initial reactive isoprene unit for the prenyl-transfer steps that lead to squalene and, hence, to cholesterol. Isomerase has been purified from *Claviceps purpurea* and *Saccharomyces cerevisiae.* The mechanism of action of the enzyme has been studied by using a series of mechanism-based covalent irreversible inhibitors, suicide substrates, and noncovalent, tight-binding inhibitors designed to mimic reactive intermediates or transition states in the isomerization. These results will be discussed in the context of a carbocationic mechanism for isomerization.

29. No abstract available.

30. Oxidatively Modified Low-Density Lipoprotein in Atherogenesis. *Sampath Parthasarathy.* Department of Medicine, M-013D, University of California, San Diego, La Jolla, CA 92093.

Adherence of monocytes to the endothelium and their penetration into the intima represent one of the earliest events in atherogenesis. These cells mature into macrophages and develop into cholesteryl ester laden foam cells. Most of the lipids found in foam cells are derived from low-density lipoprotein (LDL). The inability of macrophages to form foam cells when incubated with LDL in vitro led to the postulation that the atherogenicity of LDL may be mediated by postsecretory modifications of LDL. One such modification results when LDL is incubated with cultured endothelial cells or incubated under conditions that permit peroxidation of LDL lipids. Oxidatively modified LDL may promote atherogenesis by at least the following ways: (1) oxidized LDL is chemotactic to monocytes and may help to recruit them into the intima; (2) oxidized LDL inhibits the motility of macrophages and may prevent the efflux of mature macrophages; (3) oxidized LDL is degraded by macrophages by way of a specific receptor, resulting in cholesteryl ester accumulation; and (4) oxidized LDL causes injury to the endothelium.

THURSDAY MORNING—SYMPOSIUM ON RATIONAL TARGETS FOR HERBICIDE DESIGN (COSPONSORED WITH THE DIVISION OF AGROCHEMICALS) (SECTION B)—P. HAYWORTH, ORGANIZER, PRESIDING

Insect Cytochrome P450: New Look at an Old Target. *R. Feyereisen.* Departments of Entomology and Agricultural Chemistry, Oregon State University, Corvallis, OR 97331.

Insect cytochrome P450 monooxygenases are best known for their role in the metabolism of insecticides that leads to activation or detoxification. Insecticide synergists such as piperonyl butoxide are "classical" inhibitors of cytochrome P450 enzymes. Some lesser known cytochromes P450 metabolize the precursors of insect molting hormones, juvenile hormones, and some pheromones. As we increase our understanding about the metabolism of insect hormones and pheromones by cytochrome P450 enzymes, these endogenous functions are becoming attractive targets for specific inhibitors. Rational design of inhibitors will be aided by a molecular analysis of cytochrome P450 structure, which is made possible by the recent cloning and sequencing of cytochrome P450 genes.

Naturally Occurring Auxin Transport Regulators. *Mark Jacobs.* Department of Biology, Swarthmore College, Swarthmore, PA 19081. Philip H. Rubery. Department of Biochemistry, University of Cambridge, Cambridge, U.K.

The polar transport of the plant hormone auxin can be inhibited by a group of synthetic compounds that act by binding to a plasma membrane protein known as the naphthylphthalamic acid (NPA) receptor. No endogenous ligand for the NPA receptor, capable of affecting polar auxin transport (PAT), has previously been reported. We have found that a group of flavonoids—including quercetin, apigenin, and kaempferol—can specifically compete with [^{3}H]NPA for binding to its receptor and can perturb auxin transport in a variety of plant tissues and transport systems in a manner paralleling the synthetic PAT inhibitors. There are specific structural requirements among the flavonoids for maximum NPA-like activity. Since the active flavonoids are widely distributed in the plant kingdom and exert their effects at micromolar concentrations approximating likely endogenous levels, they may act as natural auxin transport regulators in plants.

Branched-Chain Amino Acid Catabolism by the Insect Corpus Allatum: Importance in Juvenile Hormone Biosynthesis by Lepidopterans vs Other Insect Orders. *P. A. Brindle*, D. A. Schooley, L. W. Tsai, and F. C. Baker. Sandoz Crop Protection Corporation, 975 California Avenue, Palo Alto, CA 94304.

Branched-chain amino acid (BCAA) catabolism by corpus allatum (CA) homogenates has been examined in lepidopterous vs nonlepidopterous insects. 2-Oxo-3-methylvalerate accumulates in homogenates of lepidopteran CA incubated with isoleucine, showing the presence of an active BCAA transaminase. Other metabolites, including the juvenile hormone (JH) precursors acetate and propionate, also accumulate. Homogenates of nonlepidopteran CA exhibit negligible BCAA transaminase activity. Lepidopterans utilize isoleucine as a source of propionyl-CoA and acetyl-CoA for JH biosynthesis; the propionyl-CoA is an essential precursor of the unusual ethyl-branched JHs found in this insect order. Nonlepidopterans produce only JH III. *Periplaneta americana* CA homogenate metabolizes 2-oxo-3-methylvalerate to propionate and acetate, and in experiments with intact CA the acetate incorporates into the JH III. Thus, the absence of BCAA catabolism by nonlepidopteran CA may be attributable to the lack of BCAA transaminase on an otherwise functional pathway. (Partly funded by NSF Grant DMB-8518299.)

Probing Lethal Metabolic Perturbations in Plants with Chemical Inhibition of Dehydroquinate Synthase. S. Myrvold, L. M. Reimer, D. L. Pompliano, and *J. W. Frost.* Department of Chemistry, Purdue University, West Lafayette, IN 47907.

Are all amino acid biosynthetic enzymes in plants comparably good targets for enzyme-targeted herbicides? In relation to this question, in vitro and in vivo inhibitions of an enzyme in the common pathway of aromatic amino acid biosynthesis have been examined. The enzyme dehydroquinate (DHQ) synthase is not precedented to be the target of any known herbicide. Synthesis of DHQ synthase inhibitors is discussed along with the associated inhibition of enzyme isolated from both microbial and plant sources. The impact of postemergent application of a DHQ synthase inhibitor is gauged by the buildup of the substrate of DHQ synthase in plant tissue as well as visual and growth indexes of herbicidal activity.

Mechanism of Phosphorodiamidate and Phosphoric Triamide Urease Inhibitors. *Michael D. Swerdloff*, Susan B. Anderson, Raymond J. Brambilla, and Milorad M. Rogic. Allied-Signal Corporation, Morristown, NJ 07960.

Urease inhibitors containing the diaminophosphinyl group are extremely effective in increasing the efficiency of surface-applied urea fertilizers. Evidence is presented here to suggest that these compounds inhibit urease not only by binding tightly as transition-state analogues but also by forming reversible, covalently bound phosphorus intermediates in a manner similar to cholinesterase inhibitors. 4-Nitrophenylphosphorodiamidate was shown to be a substrate for jack bean urease at pH 7.6 and to lose 4-nitrophenol at a rate directly proportional to the concentration of the enzyme. Under similar conditions, ^{31}PMR studies demonstrated that phenylphosphorodiamidate, trichloroethylphosphorodiamidate, and *N,N*-diethylphosphoric triamide were also substrates and preferentially decomposed by the loss of the organic alcohol or amine group. *N*-(*n*-Butyl)thiophosphoric triamide (NBPT), one of the most effective urease inhibitors, however, was very stable in the presence of jack bean urease under the same conditions. A mechanism to explain urease inhibition by these compounds is presented.

THURSDAY AFTERNOON—POSTER SESSION—D. SIGMAN, J. A. GERLT, J. STUBBE, PRESIDING

31. Does Phospholipase A_2 Catalyze the Hydrolysis of Monomeric Substrates? *Daniel Quinn.* Department of Chemistry, University of Iowa, Iowa City, IA 52242. Michael Gelb. Department of Chemistry, University of Washington, Seattle, WA 98195. Juan Vidal and Paul Sigler. Department of Biochemistry and Molecular Biology, University of Chicago, Chicago, IL 60637.

Below the cmc's of phospholipid (PL) substrates, phospholipase A_2 (PLA_2) displays Michaelis–Menten kinetics. However, K values usually track with the cmc's: with increasing substrate hydrophobicity both cmc and K decrease. This association suggests that Michaelis–Menten kinetics

below the cmc do not reflect turnover of monomeric substrates. The following test can be applied to gauge whether this is the case: (a) calculate K and V by fitting initial velocity data measured just below the cmc (within around 1 order of magnitude); (b) measure V/K at high PL dilution (2–3 orders of magnitude below the cmc). We will show for various PLA_2's and PL's that V/K values so measured differ significantly from those calculated from Michaelis–Menten parameters. Therefore, Michaelis–Menten kinetics below the cmc do not monitor PLA_2-catalyzed hydrolysis of PL monomers.

32. Alternate Substrate Studies of Reductoisomerase. *G. Mrachko* and K. C. Calvo. Department of Chemistry, University of Akron, Akron, OH 44325.

Ketal-acid reductoisomerase (RI) is a unique enzyme of the branched-chain amino acid biosynthetic pathway. The enzyme uses NADPH and Mg^{2+} for the conversion of α-acetolactate and α-aceto-α-hydroxybutyrate to α,β-dihydroxyisovalerate and α,β-dihydroxy-β-methylvalerate, respectively. Presumably, RI catalyzes the reduction of a ketone and performs a 1,2-alkyl migration without the aid of a coenzyme. Initial kinetic isotope studies revealed a small KIE on V/K in the forward reaction. On this occasion, our interests focus on kinetic studies of alternate substrates and their use in the partial disclosure of the enzyme mechanism. In this presentation, we describe the synthesis of several new substrates for RI (I–VIII) and present the results of product characterization and steady-state and kinetic isotope effect studies using these new substrates.

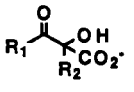

R_1=Me, R_2=Me (I), R_2=Et (II), R_2=Bz (III), R_2=CH_2OMe (IV)
R_1,R_2= -CH_2CH_2- (V), -$CH_2CH_2CH_2$- (VI) R_1=Et, R_2=Me (VII) R_2=H (VIII)

33. Cloning and Expression of Genes in the Mandelate Pathway. Stephen C. Ransom, Amy Y. Tsou, Deborah Loveys, Vincent M. Powers, George L. Kenyon, and *John A. Gerlt*. Department of Chemistry and Biochemistry, University of Maryland, College Park, MD 20742, and Department of Pharmaceutical Chemistry, University of California, San Francisco, CA 94143.

Our previously described clone of the gene for mandelate racemase from *Pseudomonas putida* [(1988) *Biochemistry 27*, 540] has been found to also contain the gene for (*S*)-mandelate dehydrogenase. A mixed oligonucleotide (38-mer) designed on the basis of the N-terminal sequence determined for benzoylformate decarboxylase (BFD) isolated from *P. putida* has been used to probe for the gene for BFD in Southern blot analyses. This probe and a 17-mer incorporating an exact portion of the sequence for mandelate racemase (MR) bind to *Eco*RI restriction fragments of approximately 9 kb in length, suggesting that the gene for BFD is closely linked to and lies upstream of the gene for MR. Further progress in characterizing and expressing the gene for BFD and in studying the chromosomal organization of the various genes encoding the enzymes in the mandelate pathway will be reported.

34. Site-Directed Mutagenesis of Cys 759 of *E. coli* Ribonucleotide Reductase. *M. I. Johnston*, S. S. Mao, and J. Stubbe. Massachusetts Institute of Technology, Cambridge, MA 02139.

Cys 754 and 759 of the B_1 subunit of ribonucleotide reductase have been postulated to be directly involved in the reduction of CDP to dCDP [Lin et al. (1987) *Biochemistry 26*, 6905]. To test this hypothesis, B_1 has been overexpressed by using the method of Tabor and Richardson for the cloning of toxic genes [Tabor & Richardson (1985) *Proc. Natl. Acad. Sci. 84*, 1074]. A Cys 759 to Ser 759 mutant was prepared according to the method of Taylor et al. [(1985) *Nucleic Acids Res. 13*, 8764]. S759 reduces CDP to dCDP at 7.7% the rate of wild-type B_1 in the presence of thioredoxin and thioredoxin reductase. With dithiothreitol as the reductant S759 reduces substrate at the same rate as wild type, at 9% of the rate using the natural reductant. Cys 759 in B_1 is therefore not directly involved in reduction of the substrate at the active site but may function by shuttling electrons from thioredoxin to the active site.

35. Site-Directed Mutagenesis of Cys 225 of *E. coli* Ribonucleotide Reductase. *M. I. Johnston*, S. S. Mao, J. M. Bollinger, and J. Stubbe. Massachusetts Institute of Technology, Cambridge, MA 02139.

The B_1 subunit of ribonucleotide reductase has been overexpressed by using the pGP1-2/pT7-5 system developed by Tabor and Richardson for the cloning of toxic genes [Tabor & Richardson (1985) *Proc. Natl. Acad. Sci. 84*, 1074]. A Cys 225 to Ser 225 mutant was prepared according to the method of Taylor et al. [(1985) *Nucleic Acids Res. 13*, 8764]. Incubation of S225 with B_2 and [U-^{14}C]CDP for 30 min results in production of 7 equiv of cytosine/S225 and covalent modification of the protein. Kinetic studies revealed that both the B_2 and S225 subunits are inactivated during this incubation. Inactivation of B_2 is the result of destruction of the tyrosyl radical. This is the first example of substrate-mediated tyrosyl radical loss. Inactivation of S225 is amazingly the result of cleavage of the protein into two pieces (M_r = 28, 60). These results can be explained in terms of a cation radical mechanism for the normal reduction process.

36. Site-Directed Mutagenesis of the Tryptophan Synthase $\alpha_2\beta_2$ Complex from *Salmonella typhimurium*. *Edith Wilson Miles*. Laboratory of Biochemical Pharmacology, National Institutes of Health, Bethesda, MD 20892.

Site-directed mutagenesis is used to explore the roles of residues which are located in the active sites of the α subunit and of the β subunit of tryptophan synthase in the three-dimensional structure of the $\alpha_2\beta_2$ complex from *Salmonella typhimurium* [C. C. Hyde, S. A. Ahmed, E. A. Padlan, E. W. Miles, and D. R. Davies (1988) *J. Biol. Chem.* (in press)]. Our finding that replacement of aspartic acid 60 of the α subunit by asparagine, alanine, or tyrosine results in complete loss of activity supports a catalytic role for aspartic acid 60 in the reversible cleavage of indole-3-glycerol phosphate. Aspartic acid 60 and glutamic acid 49 are thought to facilitate this reaction by general acid–base catalysis. Amino acid substitution of the β subunit lysine 87, which forms a Schiff base with pyridoxal phosphate in the wild-type β subunit, yields an inactive form of the β subunit which binds α subunit, pyridoxal phosphate, and L-serine. These results support a role for lysine 87 in removing the α proton of L-serine.

37. Probing the Active Site of Neutral Endopeptidase 24.11 by Site-Directed Mutagenesis. *L. B. Hersh*, R. C. Bateman, Jr., D. Jackson, and J. Vijayaraghavan. Department of Biochemistry, Southwestern Medical Center, Dallas, TX 75235.

Neutral endopeptidase 24.11 (NEP) is a metalloendopeptidase believed to function in the inactivation of a number of physiologically active peptides. The enzyme cleaves peptides

on the amino side of hydrophobic residues and in this and in other respects is similar to the bacterial enzyme thermolysin. On the basis of a comparison of NEP with thermolysin, a putative valine believed to be involved in substrate binding has been changed to a leucine residue. The effect of this substitution is to decrease k_{cat} for bulky amino acid side chains, but to have little effect with an Ala side chain. A second mutation involving the conversion of an active-site arginine to a glutamine alters the ability of the enzyme to discriminate between free acids and amides. This arginine appears to bind the C-terminal carboxylate of peptides.

38. Site-Directed Mutagenesis Studies on the Nucleotide-Metal Binding Site of *E. coli* Glutamine Synthetase. *L. M. Abell*, P. J. Keck, and J. J. Villafranca. Department of Chemistry, The Pennsylvania State University, University Park, PA 16802.

Glutamine synthetase from *E. coli* requires two divalent metal ions per active site to catalyze the ATP-dependent synthesis of glutamine from glutamate and ammonia. The protein ligands to the nucleotide-metal have been identified from X-ray crystallographic data as glutamates 129 and 357 and histidine 269 [Almassy et al. (1986) *Nature 323*, 304]. Histidine 269 provides the only nitrogen metal ligand at either metal binding site. A series of mutants has been constructed which contain potential oxygen and nitrogen ligands at position 269. When this histidine is replaced with asparagine or aspartic acid, the catalytic activity of the enzyme decreases by a factor of at least 100 and the pH optimum for catalysis shifts from pH 7.5 for wild type to 6.5 and 6.0, respectively. The metal ion dissociation constants for both metal sites have been altered by these mutations, and the effect of pH on these parameters has been investigated. The kinetic properties of these mutants have also been studied. (Supported by NIH Fellowship GM 11994-02. This work is supported by NIH Grant GM 23529.)

39. ^{1}H, ^{13}C, and ^{15}N NMR Studies of *E. coli* Porphobilinogen Deaminase. *Neal J. Stolowich*, Karen R. Clemens, Charles A. Roessner, and A. Ian Scott. Center for Biological NMR, Department of Chemistry, Texas A&M University, College Station, TX 77843-3255.

Porphobilinogen deaminase, which catalyzes the polymerization of four molecules of porphobilinogen (PBG) to form the linear tetrapyrrole hydroxymethylbilane, was investigated by using multinuclear NMR spectroscopy. As reported previously, PBG deaminase overexpressed from *Escherichia coli* was found to contain a novel dipyrromethane cofactor composed of two molecules of substrate PGB covalently linked to cysteine 242 of the enzyme. By use of ^{13}C- or ^{15}N-enriched PBG, enzyme isotopically labeled in either its cofactor or subsequent intermediate complexes can be prepared and examined by NMR. Additionally, the apoenzyme form of deaminase can be prepared and the reconstitution process of the enzyme observed by monitoring changes in substrate and protein resonances. The NMR results are discussed in terms of the structure and mechanism of PBG deaminase.

40. Reconstitution of Apoporphobilinogen Deaminase: Structural Changes Induced by Cofactor Binding. A. I. Scott, *Karen R. Clemens*, Neal J. Stolowich, Patricio J. Santander, Mario D. Gonzalez, and Charles A. Roessner. Center for Biological NMR, Department of Chemistry, Texas A&M University, College Station, TX 77843.

Porphobilinogen (PBG) deaminase (EC 4.3.1.8) catalyzes the polymerization of 4 units of PBG to form preuroporphyrinogen. This unusual enzyme is synthesized in vivo with a covalently attached dipyrromethane cofactor, derived from 2 units of its own substrate. Expression of porphobilinogen deaminase in a *hemB*$^{-}$ strain of *E. coli* has permitted the isolation of the apoenzyme lacking cofactor. Incubation of purified apoenzyme with PBG resulted in reconstitution of the dipyrromethane cofactor, indicating attachment of the cofactor requires no additional enzymes or agents during biosynthesis of the holoenzyme. Electrophoretic and ^{13}C NMR spectroscopic analyses demonstrate that the apoenzyme exists in a conformationally unstable form which assumes stable tertiary structure upon attachment of the dipyrromethane cofactor. PBG analogues used in the reconstitution process up to this time have shown a lowered ability to induce conformational change or enzymic activity. The effects of reconstitution with both PBG and analogues will be discussed.

41. ^{13}C NMR Studies of the Mechanism of Inhibition of Trypsin by Leupeptin. *Claudio Ortiz*, Howard J. Williams, Neal J. Stolowich, and A. Ian Scott. Center for Biological NMR, Department of Chemistry, Texas A&M University, College Station, TX 77843.

Leupeptin (acetyl-L-leucyl-L-leucyl-L-arginal), a potent bacteria-derived inhibitor of protease activity, has been prepared ^{13}C labeled at the aldehyde C-1 carbon. X-ray crystallography data indicate that inhibition of trypsin by leupeptin may involve formation of a stable hemiacetal complex between serine 195 hydroxyl and the arginal aldehyde. In a study using ^{13}C NMR spectroscopy of the enzyme inhibitor complex, we obtained direct evidence of the tetrahedral sp^3 configuration of the C-1 center as well as information about its stereochemistry.

42. ^{13}C NMR Investigations of Metabolism in the Perfused Rat Heart: Relative Flux of ^{13}C through Citric Acid Cyclic Pathways. *A. D. Sherry*, C. R. Malloy, and F. M. H. Jeffrey. Department of Chemistry, University of Texas at Dallas, Richardson, TX 75080, and Departments of Internal Medicine and Radiology, University of Texas Southwestern Medical School, Dallas, TX 75235.

A ^{13}C isotopomer analysis has been developed which allows measurement of relative flux through the oxidative versus anaplerotic pathways of the citric acid cycle from a single high-resolution ^{13}C spectrum. Rat hearts have been perfused with [1-^{13}C]glucose, [3-^{13}C]pyruvate, [3-^{13}C]lactate, [2-^{13}C]acetate, or [2,4-^{13}C]acetoacetate as both Langendorff and working heart preparations and ^{13}C spectra recorded at 11.75 T. The isotopomer analysis shows there is a significant variation in substrate utilization and anaplerotic flux between hearts oxidizing these substrates and between the two perfusion models. The method is a powerful and simple approach to examine metabolism in intact tissue which may have important clinical applications.

43. ^{23}Na NMR Investigations of Perfused Rat Hearts Utilizing a Novel Shift Agent: Tm(DOTP)$^{5-}$. *D. C. Buster*, A. D. Sherry, C. R. Malloy, and F. M. H. Jeffrey. Department of Chemistry, University of Texas at Dallas, Richardson, TX 75080, and Department of Internal Medicine, University of Texas Southwestern Medical School, Dallas, TX 75235.

The thulium(III) chelate of [1,4,7,10-tetraazacyclododecanetetrayl-*N*,*N*′,*N*″,*N*‴-tetrakis(methylene)]tetrakisphosphonate [Tm(DOTP)$^{5-}$] has been utilized as a ^{23}Na shift agent for investigating intracellular sodium (Na-in) in perfused

rat hearts. $Tm(DOTP)^{5-}$ is considerably more stable in vivo than the widely used $Dy(PPP)_2^{7-}$ and imparts a sizable shift to the extracellular sodium ions (Na-out) even in the presence of physiological levels of calcium. Langendorff perfused rat hearts showed no change in rhythm, coronary flow, or developed pressure when exposed to 3.5 mM $Tm(DOTP)^{5-}$ and 1 mM free calcium. A downfield ^{23}Na shift of 1.5 ppm at 11.75 T was induced in the Na-out signal in the heart spectra, sufficient to resolve and measure Na-in. Ten-minute global ischemia was associated with an increase in [Na-in] and onset of acidosis (monitored via ^{31}P NMR), both of which reversed following reperfusion.

44. Further Studies of Tyrosine Metabolism during Insect Cuticle Formation. *Howard J. Williams*, Heather J. McAuslane, John M. Lally, and A. Ian Scott. Center for Biological NMR, Department of Chemistry, and Department of Entomology, Texas A&M University, College Station, TX 77843.

A new synthesis of ^{13}C-labeled tyrosine has been developed to study the chemical changes undergone by the amino acid as it is incorporated into cuticle by a *Heliothis virescens* larva during pupation. Prepupae are injected with a solution of the labeled tyrosine, and the metabolism in solution is first observed by solution NMR in the living insect. Cuticle hardening removes the labeled compounds from solution so the ultimate fate of the label is determined by using CP/MAS methods.

45. Comparison of Cytochrome P450 Dependent Ethoxy- and Benzyloxyphenoxazone Dealkylase Activities from Rat Lung. *J. Rabovsky*, D. J. Judy, M. McPeek, V. Castranova, and W. H. Pailes. National Institute for Occupational Safety and Health, DRDS, and West Virginia University, Morgantown, WV 26505.

Properties of cytochrome P450 (P450) dependent ethoxy- and benzyloxyphenoxazone dealkylase activities (E'ase and B'ase, respectively) were examined in lung microsomes (mic) and alveolar type II cells (t_{II}) from rats pretreated with β-naphthoflavone. The activities could not be distinguished by responses to changes in pH (7.2–8.0), salt content, or osmolarity. The activities in t_{II} were increased by sonication, and each required dicumarol to inhibit quinone reductase activity. Mic B'ase, but not E'ase, was sensitive to the presence of unsubstituted aliphatic hydrocarbons. B'ase (mic and t_{II}) exhibited a nonlinear dependence of activity at low enzyme concentration. The effect of low mic or t_{II} concentration on E'ase activity was less pronounced. Linearity was restored by phospholipid. The differences between B'ase and E'ase with respect to their sensitivities toward alkanes and to the effects of low mic or t_{II} concentration may reflect differences in substrate solubility, the position of B'ase or E'ase within the membrane, or the relationship between B'ase or E'ase and components of the P450 complex.

46. Ferritin mRNA Structure in the 5′ Regulatory Region Studied with 1,10-Phenanthroline–Copper. Steven R. Sczekan, Yuh-Hwa Wang, David S. Sigman, and *Elizabeth C. Theil*. Department of Biochemistry, North Carolina State University, Raleigh, NC 27695-7622, and Department of Biochemistry, University of California at Los Angeles, Los Angeles, CA 90024.

Ferritin mRNA provides a model for mRNA function because of the dramatic changes in translation that can be analyzed in vivo or in vitro. Recently, a conserved sequence of 28 nucleotides (nt) in the 5′ untranslated region (5′UTR) has been shown to be necessary for stimulation of ferritin mRNA function by iron in vivo and for specific binding of proteins in vitro. We now show that the synthetic nuclease produced by 1,10-phenanthroline–Cu(II) and thiols in the presence of dioxygen, which has previously been used to probe DNA structure, cleaves ferritin mRNA at specific sites. Moreover, when the 5′UTR of ferritin mRNA was analyzed, the 28-nt regulatory region of conserved sequence had distinctively hypersensitive sites, providing the first evidence, to our knowledge, of a correlation between specific structural and functional features of a eukaryotic mRNA. (Supported in part by NIH Grant DK 20251.)

47. pH Dependence of the Iron Environment in Lipoxygenases. *R. A. Cowling*, D. E. Van Dyk, and M. J. Nelson. Central Research Department, E. I. du Pont de Nemours and Company, Wilmington, DE 19898.

Lipoxygenases are non-heme iron dioxygenases that catalyze the peroxygenation of unsaturated fatty acids. For example, soybean lipoxygenase 1 catalyzes the formation of 13-hydroxyperoxy-9,11-octadecadienoic acid from linoleic acid. Several spectroscopic characteristics of the enzyme and its complexes with catechols show pH dependence with a $pK \approx 7.5$. The enzyme activity shows a similar, though less well characterized, pH dependence and is greatest at pH 9. We have extended these studies to other lipoxygenases, which show maximal activity at around pH 7, to see if the pH dependences of the spectroscopic features of the enzyme complexes are correlated with the pH dependence of the activity. The catecholate and nitric oxide complexes of soybean lipoxygenase 2 at pH 7 are spectroscopically similar to those of lipoxygenase 1 at pH 9, suggesting that the irons in these two have similar electronic environments at the pH at which each is most active.

48. Pulsed EPR Studies of the Interaction of MgATP and D_2O with the Fe Protein of Nitrogenase. T. V. Morgan, J. C. McCracken, L. E. Mortenson, and J. Peisach. Center for Metalloenzyme Studies, University of Georgia, Athens, GA 30602, and Department of Pharmacology, Albert Einstein College of Medicine, Bronx, NY 10461.

MgATP binds to the Fe protein (FeP) component of nitrogenase. Reduced FeP with MgATP bound interacts with the Fe–Mo protein; subsequently, MgATP is hydrolyzed and the FeP is oxidized during N_2 reduction. There is evidence to show that the FeP undergoes conformational changes on binding of MgATP. Measurement of stimulated spin echo (SSE) spectra was employed to evaluate the possibility of ^{31}P interaction from MgATP with the Fe center of FeP. No interactions attributable to phosphorus were observed. However, FeP in the presence of MgATP showed weak ^{14}N frequency modulations of 1.0, 2.3, and 3.6 MHz (g = 1.86, 8.8 GHz). These values are slightly shifted from those for the native protein (1.0, 2.0, 3.7 MHz). This may be significant since a recent paper suggests that arginine 101 may be involved in electron transfer from FeP to FeMo protein. No apparent effect of MgATP was found on exchange rates of the water associated with FeP with D_2O using samples frozen after 2 h or 15 s of incubation. Some differences in deuterium modulation depth are noted with and without MgATP. These differences may be attributed to orientation averaging due to a change in g tensor resulting from MgATP complexing and the conformational changes accompanying it. Electric field induced shift profiles of g values of FeP from *Clostridium pasteurianum* and *Azotobacter vinelandii* are consistent with a single 4Fe center. Shift profiles for FeP are essentially

identical with FeP + MgATP profiles. This suggests that the odd crystal field parameters of the 4Fe center are not changes by binding of MgATP. The experiments undertaken are part of a long-term goal of defining interaction(s) of MgATP with the isolated components of nitrogenase and with the active nitrogenase complex. We believe these data support our model in which MgATP binds to a site on the FeP and is transported to the FeMo protein along with one or more H_2O molecules. The model suggests the association of the two nitrogenase components results in the formation of a pocket within which water associates with the components and serves as a source of protons generated when MgATP is hydrolyzed near the site of substrate reduction.

49. Studies on the Chemical Mechanism of Histidase. *William E. Running* and W. Wallace Cleland. Department of Biochemistry, University of Wisconsin—Madison, 420 Henry Mall, Madison, WI 53706.

Previously we reported the results of experiments to determine the pH dependence of the kinetic parameters of histidine ammonia lyase [Running, W. E., & Cleland, W. W. (1988) *FASEB J. 2*, A997]. Further studies with α,β,β-trideuterohistidine and D_2O have allowed us to determine $^{D}(V/K)$ = 1.16 ± 0.01 and $^{D_2O}(V/K)$ = 1.19 ± 0.08 at pH(D) 8.0. These results imply that both proton abstraction from the β-carbon of the substrate and some solvent proton sensitive step are at least partially rate determining. Carbon–nitrogen bond cleavage is at least partially rate determining as $^{15}(V/K)$ = 1.015 (pH 8.0) shows. With the trideuterated substrate, $^{15}(V/K)$ increases to 1.022, suggesting the possibility of concerted carbon–nitrogen bond cleavage and proton abstraction. Experiments to determine the pH(D) dependence of the kinetic parameters with the slow substrate 4-nitrohistidine, which shows no isotope effect when deuterated at the β-position [Klee, C. B., Kirk, K. L., & Cohen, L. A. (1979) *Biochem. Biophys. Res. Commun. 87*, 343], are under way. Nitrogen 15 isotope effect data will also be presented. (Supported by NIH GM 18938.)

50. Kinetic Mechanism of the cAMP-Dependent Protein Kinase Catalytic Subunit in the Direction of MgADP Phosphorylation. *Moon-Young Yoon* and P. F. Cook. Texas College of Osteopathic Medicine, Fort Worth, TX 76107.

The kinetic mechanism of the cAMP-dependent kinase has been determined to be random in the direction of MgADP phosphorylation by using initial velocity studies in the absence and presence of the product, phospho-Serpeptide (Leu-Arg-Arg-Ala-Ser-Leu-Gly), and dead-end inhibitors. In contrast to the kinetic parameters obtained in the direction of Ser-peptide phosphorylation, the only kinetic parameters affected by Mg^{2+} are the dissociation constants for E·phospho-Ser-peptide and E·MgADP, which are decreased by about 4-fold. The dead-end analogue MgAMPCP binds with an affinity equal to that of MgADP in contrast to MgAMPPCP, which binds weaker than MgATP. The ratio of the maximum velocities in the forward and reverse reactions is about 200, and the Haldane relationship gives a K_{eq} of (7.2 ± 0.2) × 10^2. The latter can be compared to the K_{eq} obtained by direct measurement of reactant concentrations (2.2 ± 0.4) × 10^3 and ^{31}P NMR (1 ± 0.5) × 10^3. [Supported by grants from NIH (GM 37057 and BRSG S07 RR 07195) and the Robert A. Welch Foundation (B-1031) and by a Faculty Research Grant from the University of North Texas.]

51. cAMP-Dependent Protein Kinase: Substrate Specificity of the Catalytic Subunit. *David S. Lawrence* and Mary Prorok. Department of Chemistry, State University of New York at Buffalo, Buffalo, NY 14214.

Protein kinases mediate a diverse range of biological phenomena including glycogenolysis and cell division. In addition, these enzymes have now been implicated in the molecular events that constitute carcinogenesis. The substrate specificity of protein kinases and the factors that control specificity are the key elements ultimately responsible for the biological implications of the phosphoryl-transfer reaction. As a result, we have employed small peptides to investigate the substrate specificity of the cAMP-dependent protein kinase from bovine cardiac muscle, a known serine/threonine kinase. We have discovered that the specificity of this enzyme is broad. A variety of amino acids are phosphorylated by the A-kinase, including an amino acid not found in proteins. Factors which control the phosphorylation rates of peptides containing these amino acids will be discussed. In addition, the following issues will be addressed: the design of suicide substrates, the mechanism of phosphoryl transfer, and the relationship of serine/threonine kinases and tyrosine kinases.

52. Solvent Kinetic Iostope Effects as a Probe of the NAD–Malic Enzyme Reaction. *Chung-Jeng Lai*, Sandhya R. Gavva, Paul M. Weiss, Ben G. Harris, and P. F. Cook. Texas College of Osteopathic Medicine, Forth Worth, TX 76107, and University of Wisconsin, Madison, WI 53706.

Solvent kinetic isotope effects were determined for the NAD–malic enzyme from *Ascaris suum*. With NAD as the dinucleotide substrate, inverse effects of 0.61 ± 0.05 on V/K_{malate} and 0.85 ± 0.03 on V were observed whether protium- or deuterium-labeled L-malate is the varied substrate. With 3-acetylpyridine adenine dinucleotide, the solvent effects on V/K and V with protiomalate are 0.51 ± 0.03 and 0.81 ± 0.03, respectively. The solvent effect on V in the latter case increases to 1.23 ± 0.04 with L-malate-2-*d* while that on V/K remains the same. In all cases, the primary deuterium isotope effects are the same in H_2O and D_2O. The fraction of D_2O in the reaction mixture is directly proportional to the reciprocal of V and with K/V, suggesting a preequilibrium effect with a single proton involved. The inverse isotope effect of 0.5 suggests that a sulfhydryl is deprotonated in a step prior to hydride transfer. [Supported by grants from NIH (GM 36799, GM 18938, and BRSG S07 RR 07195), a grant from the Robert A. Welch Foundation (B-1031), and a Faculty Research Grant from the University of North Texas.]

53. Synthesis and Enzymatic Analysis of an Isosteric C-1 Pyrophosphonate Analogue of Phosphoribosyl α-1 Pyrophosphate. *Gregory S. Linn*, Vernon G. S. Box, Mohit Bhatia, Charles T. Grubmeyer, and Donald L. Sloan. Department of Chemistry, City College of the City University of New York, New York, NY 10031, and Department of Biology, New York University, New York, NY 10003.

The synthesis of an isosteric analogue of phosphoribosyl α-1 pyrophosphate has been completed. The synthesis involved an Emmons–Horner reaction between the C-1 of partially blocked ribose and triisopropyl methylene bisphosphonate, which effectively replaced the C-1 hydroxyl substituent with methylene phosphonate. After separation of the resulting α and β isomers and further deblocking, phosphorylation at two sites on the α isomer yielded the required isosteric analogue. This compound was isolated as the lithium salt (below).

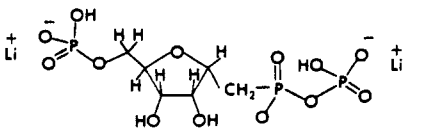

SA2434 cells containing the pCG11 plasmid were used to overproduce orotate phosphoribosyltransferase of *Salmonella typhimurium* (BOPRTase). The enzyme was purified by a four-step procedure and crystallized prior to kinetic analysis [K_m(PRibPP) = 50 ± 14 μM]. The isosteric analogue is a competitive inhibitor of the substrate PRibPP. Other phosphoribosyltransferases are being tested currently. (This work is supported by NIHRR-08168 and by the CUNY Research Foundation.)

54. Inhibition of Yeast AMP Deaminase by (*R*)-2′-Deoxycoformycin, Coformycin, and Coformycin Phosphate. *D. J. Merkler* and V. L. Schramm. Department of Biochemistry, Albert Einstein College of Medicine, Bronx, NY 10461.

Yeast AMP deaminase deaminates AMP to IMP and is activated by free ATP. Coformycin, an adenosine analogue with a tetrahedral center at the C-6 position, and related derivatives have been found to inhibit yeast AMP deaminase. Classical competitive inhibition was observed with (*R*)-2′-deoxycoformycin (K_i = 200 μM, K_M/K_i = 1). Slow-binding inhibition was observed with coformycin (K_i = 50 μM, K_M/K_i = 4) and coformycin phosphate (K_i = 60 nM, K_M/K_i = 3300). The on-rate for coformycin phosphate is $\sim 3.6 \times 10^4$ M^{-1} s^{-1}, and the off-rate is $\sim 2 \times 10^{-3}$ s^{-1}. Titrations with coformycin phosphate show that the enzyme binds one inhibitor per subunit. Previous studies have demonstrated that two ATP sites exist per subunit.

55. Yeast AMP Deaminase: Properties of Large and Small Molecular Weight Forms and Identification of the Transcriptional Start Site. *K. Kvalnes-Krick*, D. Merkler, S. Meyer, and V. Schramm. Department of Biochemistry, Albert Einstein College of Medicine, Bronx, NY 10461.

The structural gene for AMP deaminase (AMD) from *S. cerevisiae* has been cloned, sequenced, and characterized. The open reading frame of AMD corresponds to a protein of 810 amino acids (M_r 93 286). Western blot analysis of yeast extracts indicated two major bands at approximately 96 000 and 83 000 M_r, but the purified enzyme is always 83 000 M_r. The larger molecular weight form was partially purified from extracts of *E. coli* constructed to express yeast AMD. The larger molecular weight form is unstable and loses activity rapidly during purification when proteolysis is prevented. Kinetic properties of the large form were similar to those of the small form of yeast AMP deaminase. Thus, the 13 000 molecular weight N-terminal peptide of 193 amino acids is not essential for catalysis or allosteric regulation. The transcriptional start site of the mRNA encoding AMP deaminase was established by primer extension studies. RNA polymerase initiates transcription at bases 44, 35, 33, and 32 before the DNA start codon of the protein.

56. A Chemical-Enzymatic Method for the High-Yield Formation of Covalently Cross-Linked DNA. *Marlon Cowart* and Stephen J. Benkovic. Department of Chemistry, The Pennsylvania State University, University Park, PA 16802.

The modified nucleotide 6-etheno-2,6-diaminopurine-2′-deoxyribose triphosphate (6e-dDTP) was prepared by chemical

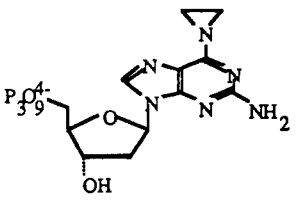

synthesis. The triphosphate is incorporated into oligonucleotides in place of 2′-deoxyguanosine triphosphate by the large fragment of *E. coli* polymerase I (Klenow fragment). The DNA template and primer strands are cross-linked concurrent with polymerization in high yield, with the N4 of a cytosine on the template strand opening the aziridine of the modified triphosphate.

57. Cell Attachment Peptides of Fibronectin and Laminin Are Chemoattractants for Endothelial Cells. *Marianna M. Long*, Vickie J. King, Kari U. Prasad, and Dan W. Urry. Laboratory of Molecular Biophysics, University of Alabama at Birmingham, Birmingham, AL 35294.

Cultured bovine aortic endothelial cells respond to a variety of chemoattractants. Among them, as we have previously shown, are repeating peptides that naturally occur in the extracellular matrix protein elastin. Dose–response experiments indicate that the concentration for stimulating maximal directed cell migration for the elastin repeat hexapeptide (Val-Gly-Val-Ala-Pro-Gly) is 10^{-8} M and for the two elastin repeat nonapeptides (Gly-Phe-Gly-Val-Gly-Ala-Gly-Val-Pro and Gly-Leu-Gly-Val-Gly-Ala-Gly-Val-Pro) is 8×10^{-10} M. Two other extracellular matrix proteins/peptides serve as chemoattractants for bovine aortic endothelial cells. They are the hexapeptide containing the cell binding sequence of fibronectin, GRGDSP, the whole fibronectin molecule itself, and the pentapeptide sequence in its amide form from laminin, YIGSR-NH_2. Dose–response curves indicate maximal activity is at 6×10^{-10}, 3×10^{-8}, and 1×10^{-8} M, respectively. Checkerboard assays demonstrated the response to be chemotactic rather than chemokinetic. (This work was supported in part by National Institutes of Health Grants HL29578 and HL41198 to D.W.U.)

58. Affinity-Directed Immobilization of Antibodies. *Russ Rines* and William H. Scouten. Chemistry Department, Baylor University, Waco, TX 76798.

Covalent immobilization of proteins to insoluble supports has been traditionally accomplished via reactive functions on the protein, usually the ε-NH_2 group of lysine. This leads to a poorly defined immobilization, since most proteins contain several lysine groups. We have synthesized several 2-fluoro-*N*-alkylpyridinium salts that contain the 2,4-dinitrophenyl (DNP) substituent. Nucleophilic hydroxyl groups on the support (agarose) displace the fluorine from these compounds, forming a reactive support. The DNP substituent functions as a hapten which attracts anti-DNP antibodies (IgG) to the support. The noncovalently bound IgG then forms a secondary amine linkage to the support via a specific lysine near the IgG hapten binding site and displaces the pyridinium as the 2-pyridone. The immobilized IgG is cleaved with a proteolytic enzyme (pepsin or papain). The fragments produced are compared (electrophoresis and HPLC) to those produced from IgG cleavage in free solution to prove that the immobilization was affinity-directed.

59. Dielectric Relaxation Studies Showing Damped Peptide Librations in D-Ala^5-PPP. *Chi-Hao Luan*, Rolf Henze, and Dan W. Urry. Laboratory of Molecular Biophysics, University of Alabama at Birmingham, Birmingham, AL 35294.

Dielectric relaxation studies on the polypentapeptide (PPP) analogue (Val^1-Pro^2-Gly^3-Val^4-D-Ala^5)$_n$ (D-Ala^5-PPP) have been carried out over a frequency range of 1 MHz–1 GHz and a temperature range of 10–60 °C. The observations demonstrate that, by means of an inverse temperature transition, a

functional state is obtained exhibiting an intense Debye-type relaxation with a relaxation time of 6 ns for D-Ala^5-PPP as previously shown for PPP. The magnitude of $\Delta\epsilon'$, previously assigned to a peptide librational process, however, was greatly reduced for D-Ala^5-PPP as anticipated from molecular mechanics calculations. The dipole moment obtained for D-Ala^5-PPP is 50–60% that of PPP. The ratio for the enthalpy of activation in kcal/mol of D-Ala^5-PPP to that of PPP is 2.6/1.2. This indicates that the barrier for libration for D-Ala^5-PPP is more than twice as great as that for PPP. The result of this study clearly supports the view that the intense relaxation near 6 ns in PPP and its analogues is due to internal chain dynamics, and the restriction of this motion results in a decrease in accessible librational states, which, in turn, results in a decrease in entropy.

60. Bradykinin and Kininogen in Bovine Milk. *W. E. Wilson*, L. H. Lazarus, and K. Tomer. LMIN and LMB, NIEHS, P.O. Box 12233, Research Triangle Park, NC 27709.

A variety of chromatographic techniques, including 13 analytical HPLC steps, were used to isolate bradykinin (BK) from milk. One microgram of BK was recovered from 18 gal of pasteurized milk; structure was determined with a gas-phase sequenator (R. Henry, Protein Lab, UNC, Chapel Hill, NC). A TPCK–trypsin digest of reconstituted dry milk yielded uterokinin equivalent to 70–80 μg of BK/L; 20–25% of this was confirmed to be BK by FAB/MS. FAB/MS analysis of a partially purified TPCK–trypsin digest confirmed that a crude commercial lactalbumin contained an appreciable quantity of bradykininogen. About 75% of pancreatic kallikrein-sensitive kininogen in pasteurized milk coprecipitated with lactalbumin prepared according to the method of Ashaffenburg and Drewry [(1957) *Biochem. J. 65*, 273–277]. Partially purified kininogen eluted from a BioSil TSK-125 column just after bovine serum albumin, suggesting a M_r = 66 000; kinin release by pancreatic kallikrein exceeded that by plasma kallikrein.

61. Selective Peptidase and Protease Activity of Platinum Complexes. Ingrid E. Burgeson and *Nenad M. Kostić*. Department of Chemistry, Iowa State University, Ames, IA 50011.

Chloro and aquo complexes of Pt(II), attached to the sulfur atom in reduced glutathione, in oxidized glutathione, and in *S*-methylglutathione, promote selective hydrolysis of the peptide bond involving the carboxyl group of cysteine. No common proteolytic enzyme cleaves next to cysteine residues. The new reagents are selective because of the stereochemical preference for the six-membered chelate ring, formed by the interaction of Pt(II) with the peptide bond. The kinetics and mechanism of this reaction and its applicability to several proteins will be discussed. A new, nonenzymic method for selective hydrolysis of proteins will be proposed.

62. Catalytic Activity of α-Chymotrypsin Tagged at the Active Site with [Pt(trpy)Cl]$^+$. *Herb M. Brothers II* and Nenad M. Kostić. Department of Chemistry, Iowa State University, Ames, IA 50011.

The complex [Pt(trpy)Cl]$^+$, shown here, is a selective and noninvasive reagent for protein modification. It labels His 57 at the active site of the proteolytic enzyme α-chymotrypsin. The stable [Pt(trpy)His]$^{2+}$ chromophore is a sensitive reporter of acid–base processes that occur in its vicinity. Even though it is platinated, the enzyme binds specific substrates and cleaves amino acid esters and amides. Strong nucleophiles remove

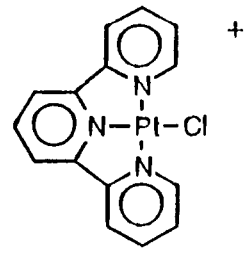

the platinum tag and restore native activity. The platinated chymotrypsin may prove useful in the synthesis of peptides that cannot be prepared with the native enzyme.

63. Epoxyalkyl-L-tyrosines: Sites and Mechanism of Inactivation of α-Chymotrypsin. *F. Jordan*, G. Tous, and F. Adebodun. Department of Chemistry, Rutgers University, Newark, NJ 07102.

Two novel classes of irreversible serine protease inhibitors have been synthesized possessing the epoxyalkyl group attached to either the phenolic oxygen or the carboxy group of L-Tyr or L-Phe. Among the former class the one with the optimal k_i/K_i ratio against α-chymotrypsin was the *N*-benzoyl-*O'*-3,4-epoxybutyl-L-tyrosine ethyl ester. Amino acid analysis indicated that this inactivator reacted at a Met side chain exclusively. Modeling of this inhibitor at the active center showed that of the two Met side chains present on this enzyme Met 180 was a much more likely site for alkylation than Met 192. Of the second class, *N*-benzoyl-L-phenylalanyl-2,3-epoxypropyl ester was found to rapidly inactivate α-chymotrypsin at micromolar concentrations. Amino acid analysis of the inactivated protein indicated no change in either Met or His content, or that of any other potentially nucleophilic side chain near the active center, and an increase in Phe, reflecting covalent modification. On the basis of all of the evidence the inhibitor was modeled into the active site. The results suggest that for the first time alkylation of Asp 102 may have been achieved. (Supported by the Rutgers Busch Fund, a Johnson and Johnson Discovery Fellowship, and the Ciba-Geigy Corp.)

64. Effects of Sulfonates on the Esterase Activity of Carboxypeptidase A. *J. L. Frye* and J. F. Sebastian. Department of Chemistry, Miami University, Oxford, OH 45056.

Recently we reported on the effect of sulfonates on the peptidase activity of carboxypeptidase A (CPA) [(1987) *Biochem. Cell Biol. 65*, 717–725]. All sulfonates studied were found to activate peptidase activity by using the short peptide substrate benzoylglycyl-L-phenylalanine (BGP). We now describe the effect of some of these modifiers on the esterase activity of CPA. For example, 2-phenylethanesulfonate (an activator of BGP hydrolysis) is an inhibitor of esterase activity using the ester substrate benzoylglycyl-L-phenyllactate. The inhibition constant K_i is 6×10^{-3} M. These results will be discussed in detail together with other activator/inhibitor systems of CPA. Implications with regard to possible mechanistic differences between peptide and ester hydrolyses catalyzed by CPA will be presented.

65. Acetylcholinesterase-Catalyzed Hydrolysis of Choline and Phenyl Esters in the Presence of Fluoride. *Alton N. Pryor* and Daniel Quinn. Department of Chemistry, The University of Iowa, Iowa City, IA 52242.

Acetylcholinesterase (AChE) catalyzed hydrolysis of *p*-methoxyphenylformate (PMPF) and acetylthiocholine (ATCh) is inhibited by fluoride. These reactions were carried out in light (H_2O) and heavy water (D_2O) to determine the inhibition

pattern of fluoride and the solvent isotope effect on K_i for fluoride inhibition. Lineweaver–Burk plots revealed that fluoride inhibits the AChE-catalyzed hydrolysis of PMPF and ATCh noncompetitively since no K_m effect was observed, but slope and V_{max} effects were manifested. Experiments indicated that there was no solvent isotope effect on K_i for fluoride inhibition. Proton inventory experiments were performed, and the results showed that deacylation of the acylated form of AChE is solely rate determining in reactions of ATCh or PMPF with fluoride catalyzed by AChE. Reactions without fluoride illustrated that both acylation and deacylation are rate determining.

66. Proton-Transfer Catalysis and Virtual Transition-State Models Describe the Mechanism of Cholesterol Esterase Catalyzed Hydrolysis Reactions. *Larry D. Sutton* and Daniel M. Quinn. Department of Chemistry, The University of Iowa, Iowa City, IA 52242.

In vivo, pancreatic cholesterol esterase (CEase) catalyzes the hydrolysis of ingested fats, allowing their absorption across the intestinal mucosa. Since the relationship between dietary fats and coronary artery disease is well established, CEase is a potential pharmacological target for inhibition in those patients at high risk of heart disease. In vitro, CEase catalyzes the hydrolysis of *p*-nitrophenyl esters via an acyl enzyme mechanism in which deacylation is the rate-determining step. Both acylation and deacylation demonstrate normal deuterium solvent isotope effects. Proton inventories (PI) for deacylation yield straight lines for all substrates tested. The acylation step for *p*-nitrophenyl esters of ≥4-carbon acids also demonstrate straight PIs. These results are consistent with single proton transfer catalysis. Proton inventories for *p*-nitrophenyl acetate and propionate are concave downward and yield commitments to proton-transfer catalysis of 0.49 ± 0.08 and 0.59 ± 0.16, respectively, which is consistent with a virtual transition-state model of catalysis.

67. Instability of N-Terminal Methoxysuccinyl Peptides. Effect on the Kinetics of Elastase. *W. B. Knight*, R. Harrison, H. Weston, and B. Green. Department of Enzymology, Merck Sharp & Dohme Research Laboratories, Rahway, NJ 07065.

The amino termini of many peptides used as probes of endoproteinases are blocked with a methoxysuccinyl group. We have explored the stability of this substitution with the elastase substrate methoxy-succ-Ala-Ala-Pro-Val-*p*-nitroanilide (VAL). VAL was incubated in 50 mM TES (pH 7.5), 500 mM NaCl, and 10% DMSO and monitored by HPLC on a CN column. VAL slowly decomposed to a species (A) with a retention time of 6.5 min (compared to 5.7 min for VAL). A second product B was observed after prolonged incubation. The retention time observed for B (4.5 min) was similar to that of succ-Ala-Ala-Pro-Ala-pNA (3.75 min). The UV–visible spectra of the degradation products were identical with that of the starting material. The kinetic parameters of elastase toward a substrate solution containing 20% A and 80% VAL were similar to those obtained with 100% VAL. When the ratio was 45:39:16 (A:B:VAL), the K_m doubled (from 0.14 to 0.28 mM). While the identity of A and B have not been established, A may be the result of intramolecular addition of the nitrogen of the terminal amide bond to the ester carbonyl, expelling methanol to produce a terminal succinimide. A may then slowly hydrolyze to produce succ-Ala-Ala-Pro-Val-pNA. Studies are under way to confirm this hypothesis.

68. Studies on the Inactivation of HMG-CoA Reductase by BDB-CoA. *Richard E. Dugan.* Lipid Research Laboratory, William S. Middleton Memorial Veterans Hospital, Madison, WI 53705.

The affinity probe *S*-(4-bromo-2,3-dioxobutyl)-CoA (BDB-CoA) irreversibly inactivates HMG-CoA reductase solubilized and purified from yeast. The reaction product is stable to dialysis and gel filtration and produces an ultraviolet spectrum consistent with CoA and protein in a 1:1 ratio. Also, the inactivation proceeds stoichiometrically at BDB-CoA/enzyme ratios less than 0.5. The inactivation is faster than with other acyl-CoA-binding enzymes, $k_3 = 4 \times 10^2$ min^{-1}. The inhibition constant is in the 10–100-μM range. The rate of inactivation is not affected by pH through the range 5.5–9.0. The substrate HMG-CoA protects against inactivation by BDB-CoA. However, mevinolin, which is believed to compete with HMG-CoA for the HMG-CoA-binding site, does not protect even at levels far above that needed to completely inhibit catalysis. This does not appear to be consistent with mevinolin inhibition via competition with HMG-CoA for its binding site.

69. Synthesis of Thiophosphatidylinositol and Stereospecificity of Phosphatidylinositol-Specific Phospholipase C. *Gialih Lin* and Ming-Daw Tsai. Department of Chemistry, The Ohio State University, Columbus, OH 43210.

(R_p)- and (S_p)-1,2-dipalmitoyl-*sn*-glycero-3-thiophosphoinositol (DPPsI) were synthesized from 1,2-dipalmitin and properly protected, enantiomerically pure 4-*O*-methoxymethyl-2,3:5,6-di-*O*-cyclohexylidene-D-*myo*-inositol, using chloro(diisopropylamino)methoxyphosphine as the phosphorylating agent. The R_p and S_p isomers were assigned on the basis of the stereospecific hydrolysis of the S_p isomer by phospholipase A_2 (it should be noted that the relative configuration of the S_p isomer of DPPsI corresponds to that of the R_p isomer of thiophosphatidylcholines). The analogues were used to test the stereospecificity of phosphatidylinositol-specific phospholipase C (PI-PLC). It was found that the PI-PLC from *Bacillus cereus* specifically converts the R_p isomer of DPPsI to D-*myo*-inositol 1,2-cyclic thiophosphate. Thus, PI-PLC shows the same stereospecificity as phosphatidylcholine-specific PLC. These results have opened the door for using stereochemistry to probe the unique mechanism of physiologically significant PI-PLC.

70. Spectral Studies of Bovine Dopamine β-Hydroxylase: Lack of Evidence for Covalently Bound Pyrroloquinoline Quinone. *James G. Robertson*, Alok Kumar, and Joseph J. Villafranca. Department of Chemistry, The Pennsylvania State University, University Park, PA 16802.

Dopamine β-hydroxylase (DβH) is a Cu^{2+}-containing monooxygenase that catalyzes the conversion of dopamine to norepinephrine. In the enzyme's initial catalytic step, ascorbate binds and reduces both Cu^{2+} to Cu^{+}. Recently it has been proposed that DβH contains covalently bound pyrroloquinoline quinone (PQQ) and that this organic cofactor may be involved in the redox functions of the enzyme in conjunction with Cu^{2+} and ascorbate (*FEBS Lett. 231*, 303). The primary evidence for this contention is the spectral identification of PQQ and PQQ–phenylhydrazine adducts in native DβH and the extraction of proteolytic products from DβH that comigrate with authentic PQQ–phenylhydrazine adducts on HPLC. We have not observed the characteristic PQQ absorption peak at ≈340 nm in native DβH, nor have we observed formation of the PQQ–phenylhydrazine adduct under turnover conditions or during overnight incubation at 40 °C. In control experiments, phenylhydrazine alone was oxidized completely within 4 h at

40 °C in 100 mM NaH_2PO_4, pH 7.0. This suggests that other chemical species may be responsible for the formation of peptide adducts that comigrate with the C(5) hydrazone of PQQ on HPLC.

71. Dietary Lipid Intake Is a Determinant of Prostaglandin E_2 Synthesis in Vivo. *A. Ferretti* and J. T. Judd. Human Nutrition Research Center, USDA, Beltsville, MD 20705. P. R. Taylor, A. Schatzkin, and C. Brown. National Cancer Institute, DHHS, Bethesda, MD 20892.

To help elucidate the biochemistry of diet-associated changes of clinical parameters, we evaluated the effect of dietary lipids on the prostaglandin system. The target biochemical marker was 7α-hydroxy-5,11-dioxotetranorprostane-1,16-dioic acid (PGE-M). In a crossover design, 24 free-living male subjects in good health (24–54 yr) were fed two diets: (i) regular (R) diet, 41% energy (en%) from fat, P/S 0.59, M/S 0.96; (ii) experimental (E) diet, 19 en% from fat, P/S 1.31, M/S 1.48. Each controlled-diet period lasted 10 weeks. The PGE-M excretion rates were determined in 24-h urine by stable-isotope dilution GC-MS. The R diet, with an intake of 9.3 en% from polyunsaturates, was associated with a higher PGE-M daily output, compared to the E diet with a 6.6 en% from polyunsaturates ($P < 0.05$). These results indicate that relatively moderate dietary lipid changes can alter prostaglandin E_2 production in vivo. We cannot conclude, however, if this diet effect was a direct result of different linoleate intakes in the two diets or of complex biochemical interactions among individual fatty acids, both saturated and unsaturated.

72. Alfalfa (*Medicago sativa*): A Source of Cholesterol Reductase. *S. S. Dehal*, J. A. Johnson, J. W. Yound, and D. C. Beitz. Department of Animal Science, Iowa State University, Ames, IA 50011.

Cholesterol (chol) reductase catalyzes reduction of chol to coprostanol (copr). Young alfalfa leaves were homogenized in a phosphate buffer (100 mM, pH 6.5) containing reducing agents, EDTA, insoluble polyvinylpolypyrrolidone, and Amberlite XAD-4. Cytosol was prepared from this homogenate and was used as the enzyme source after dialysis against phosphate buffer (5 mM, pH 6.5) containing dithiothreitol (0.5 mM) and glycerol (10%, v/v). Activity was assayed at 37 °C for 60 min with [^{3}H]chol–lecithin micelles (1 mM) and NAD(P)H (1 mM). Products were extracted with $CHCl_3$:CH_3OH (2:1, v/v); $CHCl_3$ extract was concentrated after addition of chol and copr standards. Products were separated on TLC, and radioactivity was determined. At optimal pH of 6.5, enzyme catalyzed 1% reduction of chol to copr, whereas the microsomes and boiled controls resulted in negligible reduction. NADH seems to be the preferred cofactor. Our results document the presence of chol reductase in cytosol of alfalfa leaves. (Supported in part by Wisconsin Milk Marketing Board.)

73. Mechanism of Urease Inhibitory Activity Associated with *N*-(*n*-Butyl)thiophosphoric Triamide. *Gary L. Creason*, Mark R. Schmitt, Elizabeth A. Douglass, and Larry L. Hendrickson. EniChem Americas, Inc., Monmouth Junction, NJ 08852.

N-(*n*-Butyl)thiophosphoric triamide (NBPT) has been shown in recent studies to be one of the most effective inhibitors of urease activity in soil systems. Inhibition of urease activity obtained with NBPT in several soils increased markedly during the initial hours of soil incubation. NBPT itself, however, had no detectable urease inhibitory activity when tested in a coupled enzyme spectrophotometric assay immediately after HPLC purification. An NBPT derivative generated in soil was isolated by reverse-phase HPLC, with NBPT and the derivative detected by a postcolumn system based on acid hydrolysis and phosphomolybdate complex formation. The highly active derivative was shown by mass spectral analysis to be the oxon analogue of NBPT. The concentration required for 50% inhibition of jack bean urease was the same for the pure oxon analogue and phenylphosphorodiamidate.

74. Flavopyruvate Decarboxylase: A Semisynthetic Pyruvate Oxidase or Acetolactate Synthetase? *N. Annan* and F. Jordan. Department of Chemistry, Rutgers University, 73 Warren Street, Newark, NJ 07102.

At a concentration of 1 mM, 8-(α-bromoacetyl)-10-methylisoalloxazine was found to irreversibly inactivate brewers' yeast pyruvate decarboxylase (PDC) at its active center. The 6-(α-bromoacetyl) analogue was much less effective, while the 8-acetyl and 6-acetyl derivatives gave no inhibition of any kind. The stoichiometry of interaction between the flavin analogue and PDC was determined. The enzyme-bound flavin was still reactive in redox processes (e.g., *N*-propyl-1,4-dihydronicotinamide reduced it). While the flavo-PDC was inactive in pyruvate decarboxylation leading to the usual acetaldehyde product, in the presence of electron acceptors (e.g., NAD analogues) it produced acetate. Apparently the pyruvate decarboxylating activity is not abolished in flavo-PDC; i.e., the central enamine intermediate is still being generated, but is trapped by the nearby flavin. The 2-acetylthiamin diphosphate so produced is presumably hydrolyzed in a nonenzymic process. This semisynthetic enzyme embodies aspects of two structurally related flavin-dependent pyruvate decarboxylating enzymes: pyruvate oxidase and acetolactate synthetase. (Supported by NSF and ACS-PRF grants as well as the Rutgers Busch Fund.)

75. Redox Properties of Flavodoxin from *Anabaena* 7120. *K. E. Paulsen*, M. T. Stankovich, B. J. Stockman, and J. L. Markley. Department of Chemistry, University of Minnesota, Minneapolis, MN 55455, and Department of Biochemistry, University of Wisconsin—Madison, Madison, WI 53706.

Flavodoxin from the cyanobacterium *Anabaena* 7120 is a flavoprotein dehydrogenase which interchangeably shuttles electrons with ferredoxins in photosystem I to finally reduce another flavoprotein, ferredoxin–NADP oxidoreductase. Flavodoxin *Anabaena* is reduced in an overall two-electron process. Reduction by the first electron yields a blue neutral semiquinone (ϵ_{575} = 3200 M^{-1} cm^{-1}) which can be detected spectrophotometrically at 575 nm. The second electron reduction yields the fully reduced form of the isoalloxazine ring. The oxidation–reduction potential of the couple oxidized flavodoxin/flavodoxin semiquinone was determined by using riboflavin and lumiflavin as mediator dyes. The E_m value for this couple was −0.218 ± 0.008 V at pH 7.5. The oxidation–reduction potential of the couple flavodoxin semiquinone/fully reduced flavodoxin was determined by using methylviologen as a mediator dye. The E_m value for this couple was −0.426 ± 0.006 V at pH 7.5. The pH dependence of both midpoint potentials is being explored.

76. Oxidation of POX- and ALS-Bound FAD by Ubiquinone 0. *L. M. Ciskanik* and J. V. Schloss. Central Research and Development Department, Du Pont Company, Wilmington, DE 19898.

After it was discovered that the DNA sequence encoding

E. coli pyruvate oxidase [EC 1.2.2.2 (POX)] and that encoding acetolactate synthase (ALS) are similar [Grabau & Cronan (1981) *Nucleic Acids Res. 14*, 5449], further studies suggested that the herbicide binding site of ALS and the ubiquinone binding site of POX share a common evolutionary heritage [Schloss, Ciskanik, & VanDyk (1988) *Nature 331*, 360]. Both ALS and POX have an absolute requirement for FAD; however, in the former enzyme this cofactor plays no redox role. We have determined that ubiquinone 0 (Q_0) can substitute for ferricyanide in the in vitro assay of POX with comparable activity levels. In the Q_0 and the ferricyanide assay of pyruvate oxidase activity is greatly stimulated by sodium dodecyl sulfate (SDS). The kinetic parameters of POX at pH 6, 25 °C, are 0.9 s^{-1}, 51 000 M^{-1} s^{-1}, and a K_m for Q_0 of 18 μM, in the absence of SDS, and 57 s^{-1}, 140 000 M^{-1} s^{-1}, and a K_m for Q_0 of 440 μM, in the presence of saturating SDS. The apparent K_m for SDS is 17 μM at low concentrations of Q_0 (V/K conditions) and 43 μM at high concentrations of Q_0 (V_{max} conditions). POX activity is not affected by the herbicides sulfometuron-methyl and imazaquin up to 1 mM (± SDS). After anaerobic photoreduction of ALS-bound FAD, stop-flow experiments show that half of the flavin is oxidized by Q_0 at a diffusion-limited rate (>10^8 M^{-1} s^{-1}), while the other half is oxidized at a rate of 28 200 M^{-1} s^{-1}. This slower rate is linearly dependent on Q_0 up to 0.25 mM. Current studies to determine whether ALS can carry out the Q_0-dependent reaction of POX are complicated by the fact that Q_0 is reduced by the normal product of the ALS reaction, acetolactate, at a rate of 0.05 M^{-1} s^{-1}.

77. Assay and Partial Purification of Glutaminyl Cyclase. *R. C. Bateman, Jr.* Department of Chemistry, University of Southern Mississippi, Hattiesburg, MS 39406-5043.

Glutaminyl cyclase is a recently discovered mammalian enzyme which catalyzes the cyclization of N-terminal glutamine residues to pyroglutamic acid residues in many biologically active peptides. We have developed a simple spectrophotometric assay based on the use of glutamate dehydrogenase to detect the ammonia released during the cyclization reaction. This assay can detect the release of 1–2 nmol of ammonia, is linear to at least 50% product formation, and is specific for glutaminyl cyclase. Formation of pyroglutamyl peptide product accompanying ammonia formation is observed upon HPLC analysis of the reaction products. The assay is used here in the purification of glutaminyl cyclase by ion-exchange and affinity chromatography.

78. Enzymatic Synthesis of Nucleoside Diphosphates. *Robert DiCosimo*, John Seip, Susan Fager, *John Gavagan*, Ron Grosz, and David L. Anton. Central Research and Development Department, Microbiology Group, and Engineering Department, E. I. du Pont de Nemours and Company, Wilmington, DE 19898.

Nucleoside monophosphate kinase (NMPK) from bakers' yeast was purified ca. 200-fold with 58–71% recovery of enzyme activity following salt fractionation and Mono Q FPLC. The enzyme catalyzes the reversible ($K_{eq} \cong 1$) reaction of a pyrimidine nucleoside 5′-monophosphate and ATP to produce a nucleoside 5′-diphosphate and ADP. Equilibrium mixtures of CMP, CDP, ADP, and ATP were obtained when solutions containing CMP (94 mM), ATP (95 mM), dithiothreitol (1 mM), magnesium chloride (20 mM), and 0.08 units/mL NMPK were incubated at 37 °C for 24 h at pH 7.5. The enzyme could be recovered and reused, with an observed activity half-life of ca. 2 days. Increased stability of NMPK activity was obtained by enzyme immobilization via gel entrapment (PAN 500). This enzymatic process offers an economical alternative to the chemical synthesis of NDPs.

79. Thionitrobenzoate Is a Substrate for Cysteine Synthase from *Salmonella typhimurium*. *Shinichi Hara*, Srinivas Nalabolu, and P. F. Cook. Texas College of Osteopathic Medicine, Fort Worth, TX 76107.

Cysteine synthase is a pyridoxal 5′-phosphate containing enzyme that catalyzes the synthesis of L-cysteine from *O*-acetyl-L-serine and sulfide. The enzyme has a ping-pong mechanism in which α-aminoacrylate is an intermediate. A new continuous spectrophotometric assay has been developed by using 5-thio-2-nitrobenzoate as an alternate substrate for sulfide. A difference spectrum for the thionitrobenzoate (TNB) reaction shows the disappearance of absorbance at 412 nm (TNB) with a concomitant appearance of absorbance at 320 nm (product). The product, *S*-(3-carboxy-4-nitrophenyl)cysteine (CNP-Cys), has been isolated and identified by ^{1}H NMR. The new assay was used to confirm the previously proposed ping-pong mechanism. [Supported by grants from NIH (GM 36799 and BRSG S07 RR 07195) and the Robert A. Welch Foundation (B-1031) and a Faculty Research Grant from the University of North Texas.]

80. *Salmonella* Orotate Phosphoribosyltransferase: Purification and Exchange Reactions. *Mohit B. Bhatis*, Donald L. Sloan, and Charles Grubmeyer. Biology/New York University, New York, NY 10003, and Chemistry/City College of New York, New York, NY 10031.

Orotate phosphoribosyltransferase (OPRTase, EC 2.2.4.10) catalyzes the reaction of orotic acid with phosphoribosyl α-1-pyrophosphate (PRPP) to form orotate monophosphate (OMP), a step in the de novo biosynthesis of pyrimidine nucleotides. The plasmid pCG11 directs the constitutive overproduction of OPRTase, which is readily purified to homogeneity by using a four-step scheme. The purified enzyme catalyzes a Mg(II)-dependent exchange of radiolabel between each of the two substrate–product pairs, namely, OMP–orotate and PRPP–PP_i, in the absence of the other pair. The rates of the OMP–orotate exchanges are approximately 5 μmol min^{-1} mg^{-1}. The PRPP–PP_i rates are about 5-fold faster. The kinetics for these exchanges and the results of binding experiments will be discussed. These results are indicative of a ping-pong mechanism and suggest that a catalytically relevant phosphoribosylated enzyme intermediate (E-PR) may exist.

81. Measurement of Serum Levels of B-Protein and CEA as an Indicator of Tumor Recurrence and Progression. *J. C. Morrison*, R. M. Macleod, W. D. Whybrew, and E. T. Bucovaz. Departments of Biochemistry and OB/GYN, University of Tennessee, Memphis, Memphis, TN 38163, and Department of OB/GYN, University of Mississippi Medical Center, Jackson, MS 39216.

B-Protein—present in the serum of individuals with all types of studied cancers—can be used as a general biological marker for detection of the disease. CEA, although not a general marker, is elevated by a variety of cancers. Comparative results of the two assays indicate that B-protein assay has significantly greater sensitivity; CEA has slightly greater specificity. In this study, B-protein assay detected the disease several months before it was clinically detectable. The general pattern observed was that recurrence is indicated by an elevated serum B-protein level followed by rising CEA levels.

Thus, the CEA assay serves to verify recurrence of the disease as initially indicated by elevated B-protein levels, and CEA also supports B-protein results in evaluating success or failure of applied therapy.

82. Retrospective Study Used To Evaluate the B-Protein Assay as a Cancer Management Aid. *E. T. Bucovaz*, J. C. Morrison, W. D. Whybrew, and A. W. Schweikert. Departments of Biochemistry and OB/GYN, University of Tennessee, Memphis, Memphis, TN 38163, and Department of OB/GYN, University of Mississippi Medical Center, Jackson, MS 39216.

Serum of individuals with cancer contains a specific protein named B-protein. This abnormal protein is being investigated for its effectiveness as a general biological marker for the detection of cancer. In this particular report, the B-protein assay was evaluated in a retrospective study by testing serum from patients in a cancer management program. These patients had various types of cancers, which were at different stages of progression. An in-depth clinical history of each patient was available. Review of the test results revealed that the serum titer of B-protein followed the progression of the disease. Furthermore, serum B-protein levels indicated the presence of a malignancy, in most patients, several months prior to clinical detectability.

83. Elucidation of Multiple Forms of Calcium Oxalate Crystal Growth Inhibitor. *Y. Nakagawa*, A. M. Davis, and F. L. Coe. University of Chicago, Chicago, IL 60637. T. Otsuki. Chemistry Department, Occidental College, Los Angeles, CA 90041.

Calcium oxalate crystal growth inhibitors (kidney stone inhibitor) isolated from human urine and mammalian kidneys are acidic glycoproteins and showed three or four isomers. The inhibitors were purified from bovine kidneys and separated into three fractions (A, B, and C) by using a DEAE-cellulose column eluted with a linear gradient of NaCl. P content was measured by a Fisk–Sabbarow method. P contents (μg/mg of protein) were 48.5 (A), 471 (B), and 3586 (C). The samples were also analyzed by a scanning electron microscope equipped with an X-ray microanalysis system. The results indicated the presence of Na, S, P, and Cl, and found P contents were of the same order as chemical analysis. ^{31}P NMR spectrum of fraction C was measured by using a Bruker 500 NMR spectrophotometer. The chemical shifts (ppm) were +1.7458, −0.7644, and −1.1630. After alkaline phosphatase digestion, P content reduced to 1229 and the shift of +1.7458 disappeared. Dephosphorylated inhibitor inhibited calcium oxalate crystal growth 10-fold less than the native one. After deglycosylation by glycosidases, P content was 168, and NMR showed no chemical shift. Rechromatographed dephosphorylated fraction C eluted from the DEAE-cellulose column in A and B positions.

84. Effects of Crown Ether Ionophores on Biological Systems. *Cindy La Neave*, Keith H. Pannell, James E. Becvar, Mahnaz Darvish, Tim Delmont, Ralph Kolbeck, and Robert Ginsburg. University of Texas at El Paso, El Paso, TX 79968-0153, Medical College of Georgia, Augusta, GA 30912, and Stanford Medical School, Stanford, CA 94305.

Physiological properties of macrocyclic polyethers (crowns) were investigated in our laboratories by using various biological systems to better understand the mechanism with which these compounds interact with membranes. Our interest in these interactions stems from the ability of the macrocycles to encapsulate and transport metal ions. To achieve this, we have studied such biological systems as luminous bacteria, guinea pig trachea, and human coronary tissue. Our results indicate that these macrocyclic polyethers are indeed very powerful manipulators of membrane currents essential for tissue viability. While the larger crowns reversibly inhibit bacterial luminescence, they also possess powerful vasodilation properties on smooth muscle tissue. (Supported by NIH: Area R15 HL35735, MBRS RR08012, MARC GM 08048.)

85. ATPase Reaction Energetics of *E. coli* CPS Mutant and Wild-Type Enzymes. *Leisha S. Mullins* and Frank M. Raushel. Department of Chemistry, Texas A&M University, College Station, TX 77843.

CPS from *E. coli* synthesizes carbamyl phosphate from 2 molecules of ATP, NH_3 (glutamine), and bicarbonate. The reactions catalyzed by CPS are subunit dependent with the ATP-dependent reactions occurring on the large subunit and the glutaminase reaction occurring on the small subunit. Mutation of a cysteine in the proposed active site of the small subunit abolishes the glutaminase reaction while increasing the rate of the ATPase reaction on the large subunit [Rubino et al. (1986) *JBC 261*, 11320]. The ATPase reaction energetics of the wild-type and mutant enzymes have been studied by rapid quench kinetics and positional isotope exchange (PIX) reactions. The increased ATPase reaction of the mutants is enhanced by the presence of glutamine with the rates for the wild-type, glycine, and serine mutants being 62, 230, 560 nmol of ADP min^{-1} mg^{-1} at 27 °C, respectively. The exchange rate to the chemical rate in the PIX reaction is independent of glutamine. The V_{ex}/V_{chem} is 4.4, 2.9, and 2.6 for the wild-type, Gly-269, and Ser-269, respectively. The PIX ratio decreases as the hydrolysis rate increases for the mutant enzyme. The results from the PIX and rapid quench experiments suggest that the overall energetics of the ATPase reaction change in these mutants.

86. Intravenous Pluronic F-108 Protects Red Cells from Mechanical Trauma but Does Not Alter Their Microcirculation. *J. C. McPherson, Jr.*, P. W. Paustian, Jr., D. F. Ward, R. R. Runner, and J. C. McPherson, III. Department of Surgery, Medical College of Georgia, Augusta, GA 30912, and Department of Clinical Investigation, Eisenhower Army Medical Center, Fort Gordon, GA 30905.

Pluronic F-68 (F-68) has been shown to decrease blood viscosity, and therefore it should increase blood flow in the microcirculation. Because F-68 has a short half-life, we have studied pluronic F-108 (F-108), a high molecular weight homologue of F-68. A group of 10 rats were anesthesized and shaved, and the skin blood flow was measured with a TSI LaserFlo blood perfusion monitor. An isotonic solution of F-108 (11.5 mM) (0.8 mL/100 g of body weight) was given iv (tail vein) and the blood flow measured for 6 h. Only at 1 min postinjection was there a significant increase in flow rate: control = 3.79 ± 1.37 vs 1 min = 5.12 ± 2.57, $p < 0.02$. At 3, 10, 30, 60, 240, and 360 min there was no increase in flow, p = NS. Two other groups of anesthesized rats were scalded (ca. 50% body area). Thirty minutes postburn a control group was injected with saline and the other group injected with F-108. Forty-eight hours later, the mechanical fragility of the RBCs was measured: control = 38 ± 4% vs F-108 = 24 ± 4%, $p < 0.001$. We conclude that F-108 does not change skin blood flow, but it does protect the RBC membrane from mechanical trauma.

87. Selective Interactions between DNA and H1 Histone. F.

M. Hendrickson and *R. D. Cole*. Department of Biochemistry, University of California, Berkeley, CA 94720.

Histone H1, which is thought to lock in the DNA that is coiled around the nucleosome, shows substantial selectivity in DNA binding when studied in vitro. When DNA fragments from a simian virus, SV40, generated by restriction nucleases were exposed to limiting amounts of H1 histone, it became clear that H1 had an aversion to the replication origin of the virus. This was true no matter how the fragmentation was accomplished. As a control, we showed that polylysine did not mimic H1 in its avoidance of fragments containing the origin. The aversion of H1 to the origin was also found by testing the ability of H1 to protect DNA against restriction nucleases. Intact, supercoiled SV40 DNA was complexed with H1 and challenged with restriction nucleases. A restriction site in the origin was much more vulnerable to the nuclease than other sites. This selectivity might be due to differences in flexibility of the DNA or in preferential fitting of the conformation of H1 to the conformation of DNA.

88. Mode of DNA Cleavage Reactions by [Cu(II)–PMA]$^+$, A Synthetic Analogue of Cu(II)–Bleomycin. *Samuel E. Hudson* and Pradip K. Mascharak. Thimann Laboratories, University of California, Santa Cruz, CA 95064.

As part of a synthetic analogue approach to metallobleomycins (M-BLMs), a study was undertaken to elucidate the nature of DNA cleavage reaction by [Cu(II)–PMA]$^+$, an analogue of Cu(II)–BLM. The research work included free radical generation, DNA binding, and strand scission by [Cu(II)–PMA]$^+$. In degassed phosphate buffer (pH 7.4), [Cu(II)–PMA]$^+$ was reduced by dithiothreitol and regenerated by bubbling dioxygen (>80% recovery, UV–vis spectroscopy). Similar results were obtained with ascorbic acid and 2-mercaptoethanol. When the spin trap 5,5-dimethyl-1-pyrroline *N*-oxide (DMPO) was present in such solutions, an ESR spectrum of the hydroxyl radical adduct DMPO–OH was recorded. The intensity of the ESR signal decreased with increasing pH. The signal was quenched when either superoxide dismutase (SOD) or catalase was added to the reaction mixture. Effects of the OH radical on supercoiled closed circular plasmid DNA were studied in detail. Plausible mechanisms of these DNA cleavage reactions will be discussed.

89. DNA Adducts in Medaka Exposed to Diethylnitrosamine. C. S. Giam, *T. L. Holliday*, and J. L. Williams. Texas A&M University at Galveston, Galveston, TX 77553. D. E. Hinton. University of California at Davis, Davis, CA 95616.

To evaluate exposure to diethylnitrosamine (DEN) and other alkylating carcinogens, biological endpoints are often monitored. One such endpoint is the interaction of these chemicals with DNA to form DNA adducts. This biological endpoint is of particular importance since it may be the critical initial event leading eventually to adverse effects such as tumor formation. The objective of this study was to determine if DNA adducts are formed in medaka (*Oryzias latipes*) following exposure to a carcinogen. To determine adduct formation, DNA was extracted and nucleic acid mixtures were hydrolyzed under milk acidic conditions. Hydrolysates were analyzed by HPLC using a Partisil 10 SCX column, isocratic elution with methanol/ammonium phosphate (pH 2.5), and fluorescence detection. By use of this method, O^6-ethylguanine was identified in visceral mass from medaka exposed to DEN for 24 h.

Thursday Afternoon—Symposium on Rational Targets for Herbicide Design (Cosponsored with the Division of Agrochemicals) (Section B)—P. Hayworth, Organizer, Presiding

Purification and Inhibition of α,β-Dihydroxyacid Dehydratase. *M. C. Pirrung*, C. P. Holmes, H.-J. Ha, D. S. Nunn, and D. Horowitz. Department of Chemistry, Stanford University, Stanford, CA 94305.

The α,β-dihydroxyacid dehydratase (EC 4.2.1.9, DHAD) responsible for the production of α-ketoisovaleric acid in branched-chain amino acid biosynthesis has been purified from spinach leaves. This enzyme has been used as a target for design of new inhibitors which may also have herbicidal activity by interfering with leucine, valine, and isoleucine production. Progress toward the preparation of molecules which mimic the enol intermediate will be presented, and biological data on a score of compounds will be discussed.

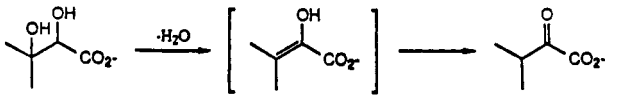

Chorismate Mutase Inhibitors: Design, Synthesis, and Evaluation of Some Potential Transition-State Analogues. *Yumi Nakagawa*, Charles R. Johnson, Siegfried H. Reich, and Paul A. Bartlett. Department of Chemistry, University of California, Berkeley, CA 94720.

The enzyme chorismate mutase catalyzes the formal Claisen rearrangement of chorismate to prephenate, a key step in aromatic amino acid biosynthesis. This transformation provides an attractive system for the study of transition-state analogue inhibition, since it is a unimolecular reaction which has an observable, noncatalyzed solution counterpart. A series of inhibitors have been synthesized which incorporate specific structural groups in a rigid framework to mimic the characteristic geometry of the proposed transition state as closely as possible. The synthesis of these inhibitors, their affinity for the target enzyme, and finally their use as templates for catalytic antibody generation will be presented.

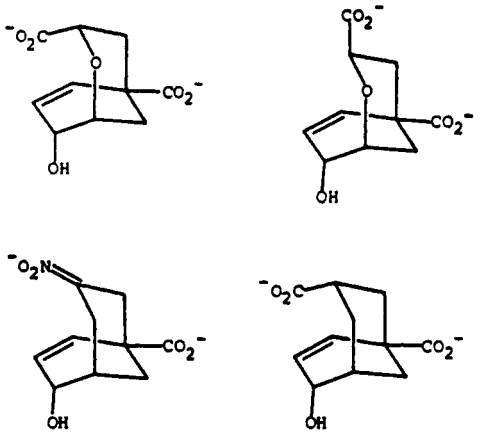

Inhibition of Early Enzymes in the Isoprenoid Pathway. *C. Dale Poulter*. Department of Chemistry, University of Utah, Salt Lake City, UT 84112.

Isopentenyl diphosphate isomerase, farnesyl diphosphate synthetase, and squalene synthetase catalyzed crucial activation and bond-forming steps in the early part of the isoprenoid pathway. Work with mechanism-based inhibitors will be

discussed which define the chemistry of catalysis for these enzymes. The compounds are highly specific and provide a range of examples of inhibitory properties, including examples of active-site-directed covalent inhibition and noncovalent tight-binding, slow-release inhibitors.

THURSDAY AFTERNOON—SYMPOSIUM ON MOLECULAR ARCHITECTURE: DESIGN, SYNTHESIS, AND FUNCTION OF SUPRAMOLECULAR STRUCTURES (CROSS-LISTED WITH THE DIVISION OF CHEMICAL EDUCATION) (SECTION C)—D. GUTSCHE, ORGANIZER, PRESIDING